

*Republic of Iraq
Ministry of Higher Education
& Scientific Research
University of Diyala
College of Science
Department of Physics*



Preparation And Studying The Physical Properties of Nano Alumina

A Thesis

Submitted to The Council of the College of Science, University
of Diyala in Partial Fulfillment of the Requirements for the
Degree of Master of Science in Physics

by

Nawar Thamer Mohammed Al-Hamdany

Supervised by

Assistant Professor Professor
Dr. Tahseen H. Mubarak & Dr. Karim H. Hassan

2014 AD

1435 AH

بِسْمِ اللَّهِ الرَّحْمَنِ الرَّحِيمِ

(فَتَعَالَى اللَّهُ الْمَلِكُ الْحَقُّ وَلَا تَعْجَلْ بِالْقُرْآنِ

مِنْ قَبْلِ أَنْ يُقْضَىٰ إِلَيْكَ وَحْيُهُ وَقُلْ رَبِّ

زِدْنِي عِلْمًا)

صدق الله العظيم

(طه:114)

DEDICATION

I DEDICATE THIS THESIS

TO MY FAMILY

TO MY WIFE

nawar

ACKNOWLEDGEMENTS

First of all I thank his Almighty Allah, Who enabled me to continue this work and overcome all difficulties

I would like to express my sincere gratitude to my supervisors Assist Prof. Tahseen Hussein Mubarak, and Prof. Karim H. Hassan who granted me the opportunity to do this research. Iam indebted to them for their suggestions and valuable remarks.

Special thanks are extended to the Dean of the College of Science and all the staff of the Department of Physics for their assistance. I would like to express my appreciation to Dr. Ziad Tariq Khuthair, for his suggestions and valuable remarks Iam also grateful to the staff Department of Materials at the University of Technology for their kind help during the laboratory work and also special thanks to the Ministry of Science and Technology for their help during the electrical tests. Also special thanks to the Dean of the Technical Institute in Baquba Dr. Karim Mubarak and all the staff of the institute , Iam also grateful to the Department of Physics at the College of Education of Ibn Al-Haytham / University of Baghdad , I would like to express my appreciation to Dr. Faleh Abdalhasan Altaie for his suggestions .

Nawar

ABSTRACT

In this study the researcher Prepared γ - alumina nanopowder were prepared using sol-gel method with a particle size 14.8 nm .The tested by XRD to measure the grain size and crystallization by comparing with card (JCPDS) files No.(46. 1215) , and SEM used to measure the particle size and shows the shape of grains and the size of porous .The physical properties such as density , porosity and hardness were studied . The Archimedes basis was used to measure the density and observed increasing in density from (1.692 g/cm³) to (1.892 g/cm³) with increasing of temperature to (350°C) and observed the porosity decrease from (6.8) to(2.06) with increase of temperature and increase in hardness from (18 GPa) to(22 GPa) with increase temperature . We studied the electrical and dielectric properties like (Dielectric constant , tangent loss , resistivity , electrical conductivity) by LCR meter with frequency from (50 Hz) to (5 MHz) . It is observed that the dielectric constant , tangent loss and resistivity decreases with the increase of frequency and electrical conductivity increases with the increase of the frequency and temperature , the dielectric strength decreases from (0.75) to(0.64) Kv/mm with the increase of temperature from(280°C) to (350°C) .

CONTENTS

Subject	Page
Chapter One: Introduction & Previous Studies	
1-1 Introduction	1
1-2 Previous Studies	4
1-3 Aims of the Study	10
Chapter Two: Theoretical Background	
2-1 Introduction	11
2-2 Alumina	11
2-3 Alumina (Aluminum Oxide) Structure	12
2-4 Mechanical properties	13
2.4.1 Bulk density	13
2.4.2 Apparent porosity	13
2.4.3. Hardness	14
2.4.4 Hardness Measurement Methods	14
2.4.5. Vickers Hardness Test	15
2.5. Electrical properties	17
2.5.1. Electrical Conductivity	17
2.5.2 Resistivity	18
2.6 Dielectrics	18
2.6.1. The principal conditions in insulator	20
2.6.2. Classification of Dielectric materials	22
2.7 Polarization	23

2.8 Types of Polarization	
2.8.1 Electronic Polarization	24
2.8.2 Ionic Polarization	24
2.8.3 Orientation Polarization	25
2.8.4 Interfacial Polarization.	25
2.9. Dielectric Properties:	27
2.9.1. Dielectric Constant	27
2. 9.2 Dielectric loss	28
2.9.3. dielectrics Temperature Dependent	32
2.9.4. Frequency dependent	33
2.9.5 Dielectric Strength	34
2.10 The Main Types of Breakdown that occur In Insulators	37
2.10.1 Intrinsic Breakdown	37
2.10.2 Electrothermal Breakdown	38
2.10.3 Electromechanical Breakdown	41
2.10.4 Streamer Breakdown	42
2.10.5 Erosion Breakdown	44
2.11 Factors Affecting on the Dielectric Strength	46
Chapter Three: Experimental Part	
3.1 Introduction	51
3.2 Raw materials	51
3.3 Tools and equipment	51

3.4 Preparation method (Sol-gel)	51
3.5 X – ray diffraction	52
3.6 Scanning electron microscope (SEM)	54
3.7 Mechanical properties	55
3.7.1 Density	55
3.7.2 porosity	55
3.7.3 Mechanical test (Hardness)	56
3.8 Electrical properties	57
3.8.1 Electrical resistivity	58
3.8.2 Electrical conductivity	58
3.8.3 Dielectric Constant	58
3.8.4 Dispersion Factor (Tangent Loss)	58
3.8.5 Dielectric Strength	59
Chapter Four: Results & Discussion	
4.1 Introduction	60
4-2 Structures Test	60
4.2.1 XRD pattern of (Al ₂ O ₃) powder	60
4.2.2 Particle size calculation from x-ray diffraction of Al ₂ O ₃	64
4-3 Scanning electron microscope (SEM) test	64
4-3-1 SEM of Al ₂ O ₃ powder prepared at 280 °C	65
4-4 Density test	67
4-5 Calculation of porosity of Al ₂ O ₃ powders at 280°C and 350°C	67

4-6 Mechanical test (Hardness)	68
4.7. Electrical properties of the alumina	69
4.7.1.The dielectric constant of alumina prepared at 280°C	69
4.7.2. Dielectric losses	71
4.7.3. Electrical conductivity	72
4.7.4.Electrical resistivity	74
4.7.5. Dielectric strength	76
4.8. Conclusions	77

LIST OF TABLES

No.	Title	Page
(1-1)	Mechanical properties	3
(1-2)	Thermal properties	3
(1-3)	Electrical properties	4
(2-1)	Main category of the types of insulators at 20°C temperature.	21
(4-1)	The location of peaks	63
(4-2)	Apparent density of alumina	67
(4-3)	Porosity of alumina	67
(4-4)	Vickers hardness test of alumina	68
(4-5)	Dielectric strength of alumina	76

LIST OF FIGURES

No.	Title	Page
(2-1)	Sketch energy Bands In The Absolute Zero temp. for insulators.	19
(2-2)	Schematic diagram for the types of Polarization.	26
(2-3)	Simplified diagram of currents in a loss dielectric.	30
(2-4)	The Relationship Between Current And Voltage In The Solid Insulators.	36
(2-5)	Mechanisms of Failure and Variation of Breakdown Strength in Solids with Time of Stressing.	37
(2-6)	draw to function ($\phi(\beta h)$), And the(x-axis) logarithmic.	39
(2-7)	Breakdown of Solid Specimen due to Ambient Discharge-Edge Effect.	42
(2-8)	Breakdown channels in plexiglass between point-plane electrodes.	44
(2-9)	Electrical discharge in cavity and its equivalent circuit.	45
(2-10)	Sequence of cavity breakdown under alternating voltages.	46
(2-11)	Effect of thickness on the dielectric strength.	48
(2-12)	Effect of temperature on dielectric strength.	49
(3-1)	XRD instrument	53
(3-2)	LCR Meter	57
(3-3)	Dielectric strength instrument	59
(4-1)	XRD patterns of Al ₂ O ₃ prepared at 280 C°	61
(4-2)	XRD patterns of Al ₂ O ₃ prepared at 350 C°	62
(4-3)	SEM images of Al ₂ O ₃ powders prepared at 280°C	65

(4-4)	SEM images of Al ₂ O ₃ powders prepared at 350°C	66
(4-5)	dielectric constant dependent on frequency applied for sample prepared at 280 C°	69
(4-6)	dielectric constant dependent on frequency applied for sample prepared at 350 C°	70
(4-7)	the variation of tangent loses with frequency for sample prepared at 280 C°	71
(4-8)	the variation of tangent loses with frequency for sample prepared at 350°C	72
(4-9)	the variation of electrical conductivity with frequency for sample prepared at 280 C°	73
(4-10)	the variation of electrical conductivity with frequency for sample prepared at 350 C°	74
(4-11)	the variation of electrical resistivity with frequency for sample prepared at 280 C°	75
(4-12)	the variation of electrical resistivity with frequency for sample prepared at 350 C°	76

LIST OF SYMBOLS AND ABBREVIATIONS

Symbol	Definition	Unit
f	Frequency	Hz
P	Polarization	C/m^2
q	Electric charge	C
N	Number of dipoles per unit volume	$1/m^3$
d	Separated distance	mm
D	Electric displacement	C/m^2
E	Electric field	V/cm
ϵ_0	Permittivity of Vacuum (8.85×10^{-12})	F/m
ϵ_r	Relative permittivity (Dielectric Constant)	---
C_0	Vacuum capacitance	F
C	Capacitance of dielectric material	F
ϵ	Permittivity of the dielectric material	F/m
P_ω	Loss power	W
V	Voltage	V
R	Resistance	Ω
I	Current	A
X_c	Impedance of capacitor	Ω
ω	Angular frequency ($2\pi f$)	$rad.s^{-1}$
j	Imaginary route, $\sqrt{-1}$	---
BD	Bulk density	g/cm^3
AP	Apparent porosity	%
δ	Loss angle	degree
ϵ'_r	Real dielectric constant	---
ϵ''_r	Imaginary dielectric constant	---
$\tan\delta$	Tangent loss angle	---

E_{br}	Dielectric field strength	kV/mm
V_{br}	Breakdown voltage	kV
h	Dielectric thickness	mm
E_o	Activation energy	
K	Boltzmann Constant	
ρ	Resistivity	

Chapter One



**Introduction
and
Previous Studies**

1.1 Introduction

Ceramic materials are generally high temperature inorganic compounds such as oxides, nitrides, carbides, boride and structurally stable system. [1, 2] Ceramics are generally classified as conventional or traditional ceramics which consist of clay and clay based materials, and high-tech or advance ceramics which are from synthetic raw materials and having specific structural and functional properties[3]. The major attraction of structural ceramics has always been the capability of operating at temperatures far above those of metals. Structural application include engine components, cutting tools and chemical process equipments. Electronic applications for ceramics with low coefficient of thermal expansion and high thermal conductivity include superconductors, substrates magnets ,and capacitors[4]. Ceramic materials can be categorized as either oxides or non-oxides and some cases may contain residual metal after some of the processing.[5,6] more oxides include alumina, silica, and mullite, alumina and mullite have been the most widely used because of their in service thermal and chemical stability and their compatibility with common reinforcements[7,8] .

1.2 Alumina

Alumina (Aluminium oxide. Al_2O_3) is mostly prepared from mineral bauxite ($\text{Al}_2\text{O}_3 + \text{SiO}_2 + \text{TiO}_2 + \text{Fe}_2\text{O}_3$) by the Bayer process which involves the selective leaching of the alumina by caustic soda followed by the precipitation of aluminium hydroxide [9]. Alumina (Al_2O_3) exists in various crystallographic forms (α , β , γ) [10] . Aluminium oxide (alumina, Al_2O_3) is currently one of the most useful oxide ceramics, as it has been used in many fields of engineering such as coatings, heat-resistant materials, abrasive grains, cutting materials and advanced ceramics. This is because alumina is hard, highly resistant towards bases and acids, allows very high temperature applications and has excellent wear resistance[11,12]. Annual demand for alumina has been growing steadily.

From an annual production of (38 million tonnes) in (1995), its reach (667 million tonnes) by the year (2005) [13,14].

Nanotechnology basically has become a key area in the development of science and the production or application of materials that have unit sizes of about (10–100) nm. Comparing micron-sized and nano-sized alumina particles, nano-alumina has many advantages. A smaller particle size would provide a much larger surface area for molecular collisions and therefore increase the rate of reaction, making it a better catalyst and reactant. Finer abrasive grains would enable finer polishing, and this would also give rise to new applications areas like nano-machining and nano-probes. In terms of coatings, the use of nano-sized alumina particles would significantly increase the quality and reproducibility of these coatings [15,16]. There are several methods to synthesize nano-alumina [17,18], and these are categorized into physical and chemical methods. Physical methods include mechanical milling, laser ablation, flame spray and thermal decomposition in plasma. Chemical methods include sol–gel processing, solution combustion decomposition and vapour deposition. Most of the chemical methods have resulted in extremely low yield rates, and thus cannot be adapted to mass manufacturing. Physical methods like mechanical milling are not efficient as the size of the nanoparticles can not be easily controlled, and these methods are only limited to certain materials. Other methods such as laser ablation, vapour deposition and sol–gel are very costly as they require specialized equipment such as vacuum systems, high power lasers as well as expensive precursor chemicals. Finally, most systems are only possible for a specific range of materials. There are researchs reports on a novel flame spray pyrolysis method to produce nano-sized alumina particles using gas and aqueous precursors. This method has many advantages over the other methods as it is low-cost, easy to

control particle size, simple processing, high production yield, and easy of conversion to mass manufacturing [19,20].

In this process, a high temperature flame is used to heat the feedstock material as well as spray it into a condensation chamber, where it will condense as nano-sized particles.

This tables (1-1) , (1-2) , (1-3) represent (mechanical , Thermal and Electrical) properties of alumina .

Table (1-1) Mechanical properties of Alumina [21]

Properties	Condition	Units	values
Bulk Density	20°C	g/cm ³	3.96
Tensile Strength	20°C	Mpa	220
Flexural (Bending) Strength	20°C	>410 Mpa	410
Elastic Modulus	20°C	Gpa	375
Hardness	20°C	Gpa	14
Fracture Toughness	20°C	Mpa*m ^{1/2}	4-5
Porosity	20°C	%	0

Table (1-2) Thermal properties of Alumina [21]

Max. working temp	-	°C	1700
Coef. Thermal Expansion	25-300°C	10-6/°C	7.8
Coef. Thermal Expansion	25-1000°C	10-6/°C	8.1
Thermal Conductivity	20°C	W/m°K	28

Table (1-3) Electrical properties of Alumina [21]

Dielectric Strength	2.5mm tk	ac-kv/mm	10
Dielectric Constant	1 MHz	-	9.7
Volume Resistivity	20°C	Ω -cm	>1014
Volume Resistivity	300°C	Ω -cm	1010
Volume Resistivity	1000°C	Ω -cm	106
Loss Factor	1 MHz	-	0.009
Dissipation Factor	1 MHz	-	0.0001

1.3 . Previous studies

A . Janbey , et., al . (2001) [22] , had prepared nano crystalline α -Al₂O₃ powders by pyrolysis of a complex compound of aluminium with triethanolamine (TEA) and sucrose . The soluble metal ion –TEA complex with sucrose forms the precursor material on complete dehydration . The single phase α -Al₂O₃ powder has resulted after heat treatment at (1150°C) . The precursor and the heat treated final powders have been characterized by X-ray diffractometry (XRD) , differential thermal and thermogravimetric analysis TG/DTA , Infrared spectroscopy (IR) and transmission electron microscopy (TEM) . The average particle size measured from X-ray line broadening and transmission electron microscopy studies are around (20 nm) . the powder which has crystallite sizes of the same order with the particle size indicates the low agglomeration of crystallites.

Cheng-Liang Huang , et., al . (2005) [23] , had studied Sintering behavior and microwave dielectric properties of nano alpha-alumina . The microstructures and the microwave dielectric properties of nano alpha alumina (α -Al₂O₃) ceramics have been investigated. It is found that the use of nano particle-sized starting material can significantly improve the densification and their microwave dielectric properties of the specimens. The α -Al₂O₃ ceramics can be sintered at

1450 °C and increased beyond 99% of its theoretical density at 1500 °C. The specimens demonstrated single α -Al₂O₃ phase throughout the entire experiments. The dielectric constant (ϵ_r) and temperature coefficient of resonant frequency (sf) were not significantly affected, while the unloaded quality factors Q were effectively promoted at temperatures higher than 1450 °C. The ϵ_r value of 10, Q_f value of 521,000 (at 14 GHz) and sf value of -48.9 ppm/°C were obtained for α -Al₂O₃ ceramics without sintering aid at 1550 °C for 4 h.

Marie K. Tripp, et al. (2006) [24], had studied The mechanical properties of atomic layer deposited alumina for use in micro- and nano-electromechanical systems. Mechanical characterization of atomic layer deposited (ALD) alumina (Al₂O₃) for use in micro- and nano-electromechanical systems has been performed using several measurement techniques including: instrumented nanoindentation, bulge testing, pointer rotation, and nanobeam deflection. Using these measurement techniques, we determine Young's modulus, Berkovitch hardness, universal hardness and the intrinsic in-plane stress for ALD Al₂O₃. Specifically, measurements for ALD Al₂O₃ films deposited at 177 °C with thicknesses between 50 and 300 nm are reported. The measured Young's modulus is in the range of 168–182 GPa, Berkovitch hardness is 12.3 GPa, universal hardness is 8 GPa, and the intrinsic in-plane stress is in the range of 383–474 MPa. Multiple measurements of the same material property from different measurement techniques are presented and compared. ALD Al₂O₃ is an advantageous material to use over various forms of silicon nitride, for micro- and nano-electromechanical systems due in part to the low deposition temperature that allows for integration with CMOS processing. Also, Al₂O₃, unlike silicon nitride, has a high chemical resistance to dry-chemistry Si etchants. Although ALD Al₂O₃ has recently been used as both a coating and a structural layer for micro and nano-electromechanical systems, its mechanical properties were not previously described.

A.I.Y. Tok , et ., al. (2006) [20] , had prepared Al_2O_3 nano-particles by flame spray pyrolysis method to synthesize agglomerate-free nano-sized Al_2O_3 particles with a size range of (5–30) nm. The precursors and the resultant oxide powders were characterized by chemical analysis, X-ray diffraction (XRD) Brunauer–Emmett–Teller (BET) analysis and transmission electron microscopy (TEM). The novel flame spray pyrolysis method successfully synthesized nano-sized Al_2O_3 of about (5–30) nm (α -phase + γ -phase), and (80–100) nm (α -phase, calcined) from AlCl_3 vapour.

Cheng-Liang Huang , et ., al. (2007) [25], had studied Microwave Dielectric Properties of Sintered Alumina Using Nano-Scaled Powders of a Alumina and TiO_2 . The microstructure and the microwave dielectric properties of nano-scaled a alumina (a- Al_2O_3) ceramics with various added amounts of nano-scaled TiO_2 have been investigated. The sintering temperature of nano-scaled a alumina can be effectively lowered by increasing the TiO_2 content. The Q_f values of nano-scaled a alumina could be tremendously boosted by adding an appropriate amount of TiO_2 . However, introducing excessive TiO_2 into the alumina ceramics would instead lead to a decrease in the Q_f values. The phases of TiO_2 and Al_2TiO_5 co-existed at 1350°C, and the maximum Q_f value appeared right after the eradication of TiO_2 phase at 1400°C. Consequently, increasing the TiO_2 content to 0.5 wt% yielded a Q_f value of 680 000 GHz (measured at 14 GHz) for nano-scaled a alumina prepared at 1400°C for duration of 4 h. In addition, a very low loss tangent ($\tan \delta$) of 2×10^{-5} was also obtained at 14 GHz. The Q_f value is strongly correlated to the compositions and can be controlled through the existing phases. In fact, Q_f could be adjusted to near zero by adding 8 wt% TiO_2 to a alumina ceramics. A dielectric constant (ϵ_r) of 10.81, a high Q_f value of 338 000 GHz (measured at 14 GHz), and a temperature coefficient of resonant frequency (sf) of 1.3 ppm/°C were obtained

for nano-scaled alumina with 8 wt% TiO₂ sintered at 1350°C for 4 h. Sintered ceramic samples were also characterized by X-ray diffraction and scanning electron microscopy.

S. Cava, et al. (2007) [26], had studied the structural characterization of phase transition of Al₂O₃ nano powders obtained by polymeric precursor method. Nano crystalline Al₂O₃ powders have been synthesized by the polymeric precursor method. A study of the evolution of crystalline phases of obtained powders was accomplished through X-ray diffraction, micro-Raman spectroscopy and refinement of the structures through the Rietveld method. The results obtained allow the identification of three steps on the (γ -Al₂O₃ to α -Al₂O₃) phase transition. The single-phase (α -Al₂O₃) powder was obtained after heat-treatment at 1050 °C for 2 h. A study of the morphology of the particles was accomplished through measures of crystallite size, specific surface area and transmission electronic microscopy. The particle size is closely related to (γ -Al₂O₃ to α -Al₂O₃) phase transition.

M. Edrissi, et al. (2007) [27], had prepared nano-powder of alumina and characterization by combustion of nitrate-amino acid gels. Nanocrystalline alumina powders were synthesized by the combustion method using serine and asparagine as fuels. A screening design was conducted to determine how key process factors influence preparation of nano crystalline powders. The screening design was utilized to rank effective factors on crystallite size of alumina powders. The product was characterized by XRD, BET, and SEM. Nanocrystalline (γ -alumina) powders with crystal sizes between (3.95 nm) and (6.71 nm) and (α -alumina) powders with crystallite sizes between (22.73 nm) and (33.92 nm) have been obtained by the combustion synthesis. The specific surface areas of samples ranged between (22 m²/g) and (75 m²/g). Particle size distributions were determined by LLS and the average particle sizes of (γ -

alumina) powders after sonication were (37.42 nm) and (79.32 nm) . Results of statistical analysis illustrate that the fuel to oxidizer ratio is the most effective factor to decrease the average crystal size .

R. Roman , et., al .(2008) [28] , had studied nano or micro grained alumina powder . Two different wet routes have been used to synthesize alumina powders in order to compare the characteristics of the final product and its behaviour during sintering. The Homogeneous Precipitation (HP) gives rise to nanoparticulated powders of about (2 nm) . However, such particles quickly aggregate and grow with calcination temperature. The Polymerized Organic-Inorganic Synthesis (POI) produces process control. Particle characterization parameters (morphology, crystallinity and degree of aggregation) are characterized by different techniques, such as DTA/TG, IR, XRD, SEM and TEM, and compared between these synthesis methods. The results show the evolution from the amorphous to the corundum alumina phase for both processes and their ability for sintering, as well discusses the beneficial of nanoparticles obtained by HP during sintering .

A . Boumaza , et., al (2009) [29], had studied the transition alumina phases induced by heat treatment of boehmite : An X-ray diffraction and infrared spectroscopy study During high temperature oxidation of alumina forming alloys, various transition aluminas are formed before reaching the most stable (α -Al₂O₃) phase. In particular, the γ , and θ transition aluminas are concerned. Precise studies on the development ,the microstructure and the properties of the oxide layers are not straight forward owing to the difficulty to unambiguously distinguish the various polymorphs by X-ray diffraction (XRD) alone .To remove this difficulty ,we propose a procedure which combines XRD and infrared (IR) spectroscopy.(γ , θ) and (α -Al₂O₃) phases, prepared by dehydration of aluminium oxihydroxide AlOOH (boehmite), were measured by XRD and IR spectroscopy on all samples. Thus, reference IR spectra were

obtained for all alumina phases, as well as an assignment of the main band in agreement with previous studies, and coherent with the structural evolution of various polymorphs. This precise characterization may constitute a basis for further investigations on thin layers of alumina formed under various experimental conditions (temperature, atmosphere, etc.).

Fatemeh mirjalili, et al. (2011) [30], had prepared nano-scale (α - Al_2O_3) powder by the sol-gel. Sol-gel method was applied to synthesize ultrafine nano (α -alumina) particles using aqueous solutions of aluminum isopropoxide and (0.5 M) aluminum nitrate hydrate. Sodium dodecylbenzen sulfonate and Sodium bis-2ethylhexyl sulfosuccinate were also used as surfactant stabilizing agents. The prepared solution was stirred for (48 hours) at (60°C), then, the resultant gelled mass was dried at (90°C), and finally, calcined at (1200°C) for about (1 hour). The samples were characterized by different techniques such as, Brunauer-Emmet-Teller method, X-ray diffraction, Thermogravimetry analysis, Differential Scanning Calorimetry, Fourier transform infrared spectra, Scanning electron microscopy and Transmission electron microscopy. The results indicated that the addition of sodium dodecylbenzen sulfonates and sodium bis-2ethylhexyl sulfosuccinate not only affected the particle size and shape of the produced nanoparticles but also the degree of aggregation. However, sodium dodecylbenzen sulfonate produced better dispersion and finer particles, in range of (20-30) nm, compared to Sodium bis-2ethylhexyl sulfosuccinate.

M. R. Karim, et al. (2011) [31], had studied and synthesis (γ -alumina) particles and surface characterization. Alumina was synthesized *via* sol-gel technique by the hydrolysis of aluminium ion controlled by urea in aqueous media. The resulting sol composed of $\text{Al}(\text{OH})_3$ particles coalesced and became a transparent gel. The freshly prepared gel was heated at (280°C) to obtain

alumina particles. The obtained particles were found to be amorphous (γ -alumina) particles with high porosity, characterized by FTIR, XRD and SBET techniques. Electron micrograph shows that the particles are nano-sized having non-spherical shape. Comparatively higher magnitude of adsorption of cationic surfactant indicated that the surface of alumina particles is negatively charged.

Rodica rogojan , et .,al .(2011) [32] , had studied synthesis and characterization of alumina nano-powder obtained by sol-gel method . It is known that sol-gel method is an alternative method to produce ceramic powders. The present study deals with the synthesis and characterization of Al_2O_3 nanopowders which can be a potentially utilized material for biocompatible implants.[1-4] Based on sol-gel method, the synthesis started from different chemical nature precursors – inorganic (aluminum chloride, AlCl_3) and organic (aluminum triisopropylate, $(\text{C}_3\text{H}_7\text{O})_3\text{Al}$). The powders obtained after drying the gel were heat treated at (1000°C) and (1200°C) for (2 hours). X-ray diffraction was used in order to characterize the powders in terms of their crystallinity degree and crystallite size. Microstructural and morphological characterization was performed using electron-microscopic techniques - scanning electron microscopy (SEM) and transmission electron microscopy (TEM) .

Omid Rahman pour,et.,al .(2012) [33] , had studied a new method for synthesis nano size (γ - Al_2O_3) catalyst for dehydration of methanol to dimethyl Ether . The materials in nano-scale show different characteristics in comparison with their bulk state . Nano-size porous (γ -alumina) was successfully synthesized by precipitation method under ultrasonic vibration mixing . chemistry help the nano particles to synthesis regular form . the synthesized catalyst characterized by SEM , XRD , BET , and TPD .

Sarojini Swain , et., al. (2012) [34] , had studied Effects of Nano-silica/Nano-alumina on Mechanical and Physical Properties of Polyurethane Composites and Coatings . the use of nano-silica / nano-alumina in polyurethane (PU) matrix, which lead to significant improvements in the mechanical and thermal properties of the nano-composite. It is observed that with incorporation of 1% of nano-alumina into the PU matrix, there is an improvement in the tensile strength of around 50%, and for nano-silica the improvement is around 41%, at the same concentration. The morphological data shows that above 3% of the nano particles there are agglomerations in the nanocomposite. Again with the absorption of moisture, there is a decrease in the thermal and mechanical properties of the PU resin, but in this research work it is observed that with the incorporation of the nano particles, in the presence of absorbed moisture there is an improvement in mechanical and thermal properties of the composite, over that of the PU matrix.

Wenhu Yang , et ., al.(2012) [35] , had studied Effect of Particle Size and Dispersion on Dielectric Properties in ZnO/Epoxy Resin Composites . In this paper, ZnO-Epoxy nanocomposites (NEP) were prepared and epoxy composites that contain 5 wt% micro ZnO (MEP) and deliberately not well dispersed nano ZnO (NDNEP) were also prepared for purpose of comparison. The effects of the particle size and dispersion of ZnO on dielectric properties of epoxy resin were chiefly studied . Test results showed that: at a loading of 5 wt%, the three epoxy composites seem to have no significant difference on resistivity compared to epoxy resin; Dielectric constants of all the epoxy composites are also basically the same but they are bigger compared to that of the pure epoxy resin (unfilled); Dielectric dissipation factors ($\tan\delta$) of NDNEP is greater than that of NEP and MEP. NEP has the minimum dielectric loss factor, whereas dielectric loss factors of the three epoxy composites are larger than that of the pure epoxy resin. The decreasing order of electrical breakdown strength for the three epoxy composites and for the pure epoxy resin is as follows: NEP>MEP>NDNEP>EP.

Finally, in order to explain the experimental results the aggregation interface phase was proposed. Furthermore, addition of well dispersed nano filler has proved to have a positive effect on the improvement of the dielectric properties of epoxy resin.

Akash Mohanty , et ., al.(2013) [36] , had studied Dielectric breakdown performance of alumina/epoxy resin nanocomposites under high voltage application . Epoxy/alumina nanocomposites were prepared by reducing micron size alumina into nanosize during the casting process. In our current investigation it was found that, at low concentration alumina nanoparticles exhibit uniform dispersion of alumina nanoparticles in epoxy nanocomposite while at higher concentration they depict aggregation of alumina particle. Since uniform dispersion of alumina nanoparticles results in improved thermal stability and viscoelastic behavior. It leads to remarkable improvement in breakdown voltage, and breakdown time of epoxy/alumina nanocomposites as compared to neat epoxy. Epoxy nanocomposites containing 2 wt.% of alumina particles results in increase of breakdown voltage by 91% and breakdown time by 155% as compared to neat epoxy. Hence, the nanocomposites developed can be used as insulating material in electrical instruments which require high breakdown voltage as well as improved viscoelastic behavior and thermal stability.

K.G. Kalpana Sarojini , et ., al.(2013) [37] , had studied Electrical conductivity of ceramic and metallic nanofluids . An extensive experimental evaluation of electrical conductivity of nanofluids containing metallic and ceramic particles (Cu, Al₂O₃, and CuO) with different volume fractions in the dilute regime, particle sizes, electrolyte effect, temperature and base fluids has been carried out. It is observed that, in both water and ethylene glycol (EG)-based nanofluids, the electrical conductivity increases with increasing particle concentration and reducing particle size. It is argued that the effective dielectric constant and density are at the root of the counterintuitive observation that the

electrical conductivity enhancement of ceramic nanofluids is more than that of metal-based ones which is substantiated by the Clausius–Mossotti relation for the polar fluids. The influence of surfactant is found to increase the stability and decrease the electrical conductivity of the nanofluids by increasing its viscosity. There is a rise in electrical conductivity of nanofluids having low electrolyte concentration whereas a decrement is observed in nanofluids of high electrolyte concentration due to reduced surface conductance. These experimental observations on alumina nanofluids are compared with the theoretical model proposed by O'Brien . for electrical conductivity of dilute suspensions. It has also been observed that there is no significant effect of fluid temperature on the electrical conductivity in the range 30–60 °C. This clearly indicates that enhancement mechanism for electrical conductivity is completely different from that of thermal conductivity in nanofluids .

1.3 Aims of the Study

Preparation of (γ -alumina) with nano size particle , Studying the mechanical properties (Density, porosity and Hardness) for the prepared alumina and the effect of temperature on these properties and the dielectric properties (dielectric constant , tangent loss , electrical conductivity , electrical resistivity, Dielectric strength and break down voltage) and the effect of frequency and temperature on these properties .

Chapter Two



**Theoretical
Background**

2-1 Introduction

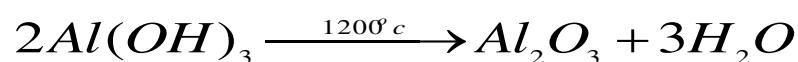
This chapter shows the theoretical part which includes the explanation of (mechanical , electrical and Dielectric) properties .

2.2 Alumina

Alumina (Al_2O_3) or aluminium oxide is the only oxide formed by the metal Aluminium and occurs in nature as the minerals corundum (Al_2O_3) ; diaspore ($Al_2O_3 \cdot H_2O$) ; gibbsite ($Al_2O_3 \cdot 3H_2O$) ; and most commonly as bauxite, which is an impure form of gibbsite .

The importance of Alumina is two –fold ;it is used as a starting material for the smelting aluminium metal , and used as a raw material for abroad range of advanced ceramic products and as an active agent in chemical processing .("Alumina" Britannica) Although the naturally occurring corundum , ruby and sapphire and sometimes also referred to as Alumina but the proper use of the term is limited to the material that is derived from bauxite and employed in the production of aluminium industrial ceramics , and chemical processing [38]

This is (Al_2O_3), which is called corundum (aluminum oxide crystalline) as an extra material in metamorphic rocks such as marble and igneous rocks, rich and poor aluminum such as cyanide, due to the hardness of the material and not influence by the weather is often concentrated in the form of granules are carried in rivers streams and on the shores of the sea [39]. The bauxite (aluminum hydroxide) ($Al_2(OH)_6$) main raw material that we get alumina from it. As contain rate alumina (40-68) % as well as varying proportions of impurities (Fe_2O_3 , SiO_2 , TiO_2) that commonly used in multiple applications in ceramics and refractories [40,41]. Alumina prepares from bauxite heated by high temperature, as follows: -



Aluminum oxide (Al_2O_3), which is called alumina is a crystalline powder, white color, density (3.9 g/cm^3). Its melting point of ($2055 \pm 6^\circ\text{C}$), does not dissolve in water or acid and is used as itchy as it comes after the diamond in hardness. Furthermore, it is a good insulator of electricity. Its energy gap ($E_g > 8\text{eV}$) [62-64]. The dielectric strength (30kV/mm) if the purity (99.7%) and contain ($\text{MgO } 0.5\%$), and (18kV/m) if the purity (97%) and contain silicate [42].

Alumina is one of the most widely used thermal oxides due to the high resistance to heat, mechanical durability and resistance to thermal shock [43]. It is used to form many articles such as spark plug cores, laser tubes, electrical insulators, thermocouple tubes, thread guides, valve seats, medical prosthesis, electronic substrates, grinding media, and many other products.[44] Mainly because of proliferation of preparative methods and the range of calcining temperature, many forms of alumina have been described. These mainly refer to partially dehydrated and improve forms that are basically ternary oxides. Pure alumina, ($\alpha\text{-Al}_2\text{O}_3$), has a hexagonal close packed structure. Other forms such as ($\beta\text{-Al}_2\text{O}_3$) and ($\gamma\text{-Al}_2\text{O}_3$) precedes the α -form during calcinations of gibbsite. Generally, The typical characteristics of alumina include: good strength and stiffness, good hardness and wear resistance, good corrosion resistance, good thermal stability, Excellent dielectric properties. and law dielectric constant and loss tangent [45,46].

2.3. Alumina (Aluminum Oxide) Structure

The structure of Aluminum Oxide has two types of sites, *hexagonal* and *octahedral* in which it holds the atoms. Hexagonal sites are the corner atoms in the cell while the octahedral sites are present between two layers of vertical stacking. Aluminum cations are in ($2/3$) of the octahedral sites, and oxygen anions are in ($1/3$) of the octahedral sites. Each oxygen is shared between four octahedra. The oxygen presence in octahedral sites permits strong bonding and, therefore, gives rise to the characteristics of the properties of alumina [38]

2.4. Physical properties (Density , porosity)

Archimedes Principle states that the buoyant force on a submerged object is equal to the weight of the fluid that is displaced by the object.

Bulk Density (BD) and apparent porosity (AP) can be measured using the Archimedes buoyancy technique from dry weights, soaked weights and immersed weights in water (mercury, xylene or denatured alcohol if the refractory is water sensitive) [47]

2.4.1 Bulk density

Apparent Density (BD) is mass divided by bulk volume where bulk volume is the volume of solid and of open and closed porosity. Bulk density can be calculated as follows [48]:

$$\text{Bulk density} = M / V \text{ (gm/Cm}^3\text{)}$$

$$\text{BD} = W_D / (W_S - W_I) \dots\dots\dots(2-1)$$

2.4.2. Apparent porosity and water absorption

Apparent Porosity (% AP) is open pore volume as a percentage of bulk volume.

The Apparent Porosity calculated from the Dry, Soaked and Suspended weights [48] as follows:

$$\% \text{ AP} = (W_S - W_D) \times 100\% / (W_S - W_I) \dots\dots\dots(2-2-A)$$

$$\text{Water absorption} = (W_S - W_D / W_D) \times 100\% \dots\dots\dots(2-2-b)$$

Where :

W_D : dry weight (gm)

W_S : soaked weight , W_I : suspended weight

2.5. Mechanical properties(hardness)

We can define hardness as "Resistance of material to plastic deformation, usually by indentation. However, the term may also refer to stiffness or temper, or to resistance to scratching, abrasion, or cutting. It is the property of a metal, which gives it the ability to resist being permanently, deformed (bent, broken, or have its shape changed), when a load is applied. The greater the hardness of the metal, the greater resistance it has to deformation.

In mineralogy the property of matter commonly described as the resistance of a substance to being scratched by another substance. In metallurgy hardness is defined as the ability of a material to resist plastic deformation.

The dictionary of Metallurgy defines the indentation hardness as the resistance of a material to indentation. This is the usual type of hardness test, in which a pointed or rounded indenter is pressed into a surface under a substantially static load .

2.5.1. Hardness Measurement Methods

There are three types of tests used with accuracy by the metals industry; they are the Brinell hardness test, the Rockwell hardness test, and the Vickers hardness test. Since the definitions of metallurgic ultimate strength and hardness are rather similar, it can generally be assumed that a strong metal is also a hard metal. The way the three of these hardness tests measure a metal's hardness is to determine the metal's resistance to the penetration of a non-deformable ball or cone. The tests determine the depth which such a ball or cone will sink into the metal, under a given load, within a specific period of time. The followings are the most common hardness test methods used in today`s technology:

1. Rockwell hardness test
2. Brinell hardness
3. Vickers
4. Knoop hardness
5. Shore .

2.5.2. Vickers Hardness Test

It is the standard method for measuring the hardness of metals, particularly those with extremely hard surfaces: the surface is subjected to a standard pressure for a standard length of time by means of a pyramid-shaped diamond. The diagonal of the resulting indentation is measured under a microscope and the Vickers Hardness value read from a conversion table .

Vickers hardness is a measure of the hardness of a material, calculated from the size of an impression produced under load by a pyramid-shaped diamond indenter. Devised in the (1920s) by engineers at Vickers, Ltd., in the United Kingdom, the diamond pyramid hardness test, as it also became known, permitted the establishment of a continuous scale of comparable numbers that accurately reflected the wide range of hardness found in steels.

The indenter employed in the Vickers test is a square-based pyramid whose opposite sides meet at the apex at an angle of (136°) . The diamond is pressed into the surface of the material at loads ranging up to approximately(120 kilograms-force), and the size of the impression (usually no more than 0.5 mm) is measured with the aid of a calibrated microscope. The Vickers number (HV) is calculated using the following formula:

$$V.H = \frac{F}{d^2/2 \sin \frac{1}{2}(136^\circ)} \dots \dots \dots (2 - 3)$$

$$H.V = 1.854(F/d^2)$$

H.V : Vickers Hardness

with F being the applied load (measured in kilograms-force) and d^2 the area of the indentation (measured in square millimetres). The applied load is usually specified when HV is cited.

The Vickers test is reliable for measuring the hardness of metals, and also used on ceramic materials. The Vickers testing method is similar to the Brinell test. Rather than using the Brinell's steel ball type indenter, and have to calculate the hemispherical area of impression, the Vickers machine uses a penetrator that is square in shape, but tipped on one corner so it has the appearance of a playing card "diamond". The Vickers indenter is a (136 degrees) square-based diamond cone, the diamond material of the indenter has an advantage over other indenters because it does not deform over time and use. The impression left by the Vickers penetrator is a dark square on a light background. The Vickers impression is more easily "read" for area size than the circular impression of the Brinell method. Like the Brinell test, the Vickers number is determined by dividing the load by the surface area of the indentation ($H = P/A$). The load varies from (1–120) kilograms. To perform the Vickers test, the specimen is placed on an anvil that has a screw threaded base. The anvil is turned raising it by the screw threads until it is close to the point of the indenter. With start lever activated, the load is slowly applied to the indenter. The load is released and the anvil with the specimen is lowered. The operation of applying and removing the load is controlled automatically.

Several loadings give practically identical hardness numbers on uniform material, which is much better than the arbitrary changing of scale with the other hardness machines. A filar microscope is swung over the specimen to measure the square indentation to a tolerance of plus or minus (1/1000) of a millimeter. Measurements taken across the diagonals to determine the area, are averaged. The correct Vickers designation is the number followed "HV" (Hardness Vickers). The advantages of the Vickers hardness test are that extremely

accurate readings can be taken, and just one type of indenter is used for all types of metals and surface treatments. Although thoroughly adaptable and very precise for testing the softest and hardest of materials, under varying loads, the Vickers machine is a floor standing unit that is rather more expensive than the Brinell or Rockwell machines [49]

2.6. Electrical properties

The electrical properties of substances play an important role in many electrotechnical applications. The factors that have the most influence on these properties are the purity of the constituent oxides and the effect of impurities on the final product, the proportions and homogeneity in the powder mix and the control of temperature [50].

2.6.1. Electrical Conductivity

This section deals with response of ceramics to the application of a constant electric field and the nature and magnitude of steady-state current that is proportional to a material property known as conductivity. In metal, free electrons are solely responsible for conduction. In semiconductors, the conducting species are electrons and/ or electron holes. In ceramics, however, because of presence of ions, the application of electric field can induce these ions to migrate. Therefore, when dealing with conduction in ceramics, one must consider both the ionic and the electronic contributions to the overall conductivity. The proportionality constant (σ) is the conductivity of material, which is the conductance of a cube of material of unit cross section [51]. The electrical properties of ceramics depend on the charge transport among B-site ions.

2.6.2 Resistivity

High resistivity ceramics with low eddy current losses are required from the technological applications point of view. The electrical resistivity of ceramics has been normally found to increase on doping or substituting with other oxides occurring at high frequencies in ferromagnetic materials[52]. This resistivity varies with applied field, temperature and frequency. Generally for ceramics materials, it decreases slightly as frequency increases. The characteristic tables of the materials indicate the mean DC - resistivity values for the various ceramic materials measured at low frequency and with a low field by using the formula [53].

$$\rho = R \frac{A}{h} , \sigma = 1/\rho \dots\dots\dots(2-4)$$

where (R) is electrical resistance, (A) represents the surface area, and (h) is the thickness of the model, (σ) represent the electrical conductivity .

The resistivity depends on temperature as in the relationship [55].

$$\rho = \rho_o \exp(E_o/kT) \dots\dots\dots(2-5)$$

where E_o activation energy, T temperature, k is the Boltzmann constant ($k = 8.62 \cdot 10^{-5} \text{ eV} \cdot \text{K}^{-1}$) and (ρ_o is a constant).

2.7. Dielectrics

A dielectric material is a non-conducting substance whose bound charges are polarized under the influence of an externally applied electric field [54]. Materials have low electrical conductivity. and use insulators to prevent the flow of the voltage to places that are undesirable or dangerous [55]. The (Article dry wood, glass, plastics, rubber and ceramics) are some examples of insulators. Also dry air and oil to be used as dielectric. Separation voltage passes with difficulty because the stick electrons to the nuclei to the extent they cannot move freely from one atom to another. So when connected to the separation electrical

moves electrons through the barrier sufficient to produce the current. According to the theory of energy bands for solids, a bundle valance band (V.B) be completely filled in the absolute zero temperature. The Energy gap (E_g) between the Valance band and the Conduction band, as show in the figure (2-1):

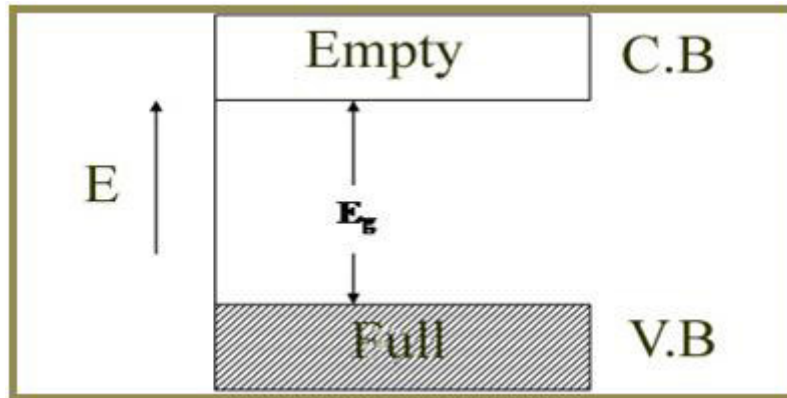


Fig. (2-1) Sketch Energy Bands at the Absolute Zero Temperature for dielectric.[55]

The depth (energy difference) of this gap may be (10eV) and above, where even if it is to applied an electric field, the electrons do not move a large number in one direction, each electron is moving towards a certain to reverse invert another electron is moving in the opposite direction of movement because the band is completely filled, such as these materials are called (Dielectrics). The energy gaps of insulators vary from material to material, In general, any material where the forbidden zone thickness is equal to more than (6 eV) be an insulator [55]. It is worth mentioning that the dielectric consists of a positive charge and the other negative and often center of negative charges applying on positive charge center of these molecules, but when there are these particles under the effect of an outside electric field, the positive charge will be displaced in the direction of field while the negative charges displaced in the opposite direction, as a result, the Center of positive charge is no applying on the center of negative charges, but separated by a small distance and then say that the molecule has become

induced dipole moment (polarized) [56]. But if the electric field is very large, this could lead to the acquisition of electrons of energy for conduction and so insulation broken [55,57].

2.7.1. The main principal conditions of dielectric are :

1. Having a high dielectric strength enough to withstand the electric field between the conductors poles .
2. Having good resistance to movement of the spark spin-off to prevent damage in the curved electric spark.
3. Having a high insulation resistance to prevent current leakage through the conductors.
4. Being consistent under different extensive environmental conditions.
5. Having sufficient mechanical properties to resist vibrations, shocks and other mechanical force.

Main classification for the types of dielectric at the temperature can be made clear in table (2-1):

Table (2-1) Main category of the types of dielectrics at 20°C [58,59]

Dielectrics Materials	Examples
Ceramic	Alumina, porcelain, Diamond,....etc.
Glass	Soda Lime, Pyrex,....etc.
Elastomer	Butyl,Natural Rubber, Polyurethane, etc.
Mica	
Paper (dry)	
Polymer	Acrylic, cellulose, Acetate, Melamine, Polyethylene (high density, low density), Polyvinyl chloride (rigid, flexible),...etc.

dielectrics are used in many kinds of electrical and electronic equipment for example, covering wire and wire bands that conduct electricity from generating stations to homes and offices by dielectric materials to prevent the current leakage. and use of insulators also capacitors to increase its capacity to store electric charge. When working in the field of equipment with high voltage, used electrical tools with handles, plastic or rubber and wear shoes with rubber soles in order to avoid damage caused by electrical shock [55].

2.7.2. Classification of Dielectric materials:

Through the relationship between the electric field and polarization dielectric materials can be classified to:

1- Permanent Polarization: Materials that are polarized in the absence of the electric field [60].

2- Linear Dielectric: include the materials that do not change the ability of the material for electrification and permittivity with polarization and intensity of the electric field, and each of the permittivity and electrification ability function of the position and divided into: -

A-Linear Isotropic Dielectric: although the electrification ability and permittivity do not depend on polarization and the electric field, there is a similarity in the trends, the applicability of any asymmetric electrifying and permittivity of the corresponding directions are equal, but they can remain dependent on the position [61].

B-Linear Isotropic Homogeneous Dielectric: These materials have the same qualities of insulators in the category (a) In addition, these materials do not depend on any position that the change in permittivity and electrifying scalability for the position is equal to zero [60].

3-Non-Linear Dielectric: Substances that have the existence of a functional relationship between electric field and electrical displacement and constants (the ability of the material for electrifying and permittivity), and the relationship between them is sometimes complex, the ceramics are located within this category, and include this insulations properties are: Ferroelectric, Piezoelectric property [62,63].

2.8. Polarization

Dielectrics have very few free electrons to take-part in normal electrical conductivity. Such a material has interesting electrical properties because of the ability of an electric field to polarize the material to create electrical dipole, thus dielectric material moleculars are called (Non polar molecules) [64,65]. As well as appearing dipole in a material in the presence of a field, dipoles may be present as a permanent feature of the molecular structure.

Such dipoles are called (Permanent dipoles) in which the center of the positive charge does not coincide with the center of the negative charges such dielectric material molecular are called (polar molecules). Induction of the dipoles is called electric polarization [66].

Phenomenon of polarization (P) down to the change in the arrangement of electrically charged particles of a dielectric in space, or is the surface charge density in a dielectric, equal to the dipole moment per unit volume of material being defined as follow:

$$P = Nm \quad \dots(2-6)$$

where:

N : is the number of dipoles per unit volume.

m : is the average dipole moment.

The electric dipole moment corresponds to two electric charges of opposite polarity $\pm q$ separated by the distance (d)[67]:

$$m = qd \quad \dots(2-7)$$

We can represent the electrical displacement (D) as the sum of the electric field (E) at a given point of dielectric and the polarization at the same point:

$$D = \varepsilon_0 E + P \quad \dots(2-8)$$

Where:

ε_0 : is the permittivity of vacuum (8.85×10^{-12} F/m)

The relationship between the electrical displacement and the electric field through a dielectric medium is:

$$D = \varepsilon_0 \varepsilon_r E \quad \dots(2-9)$$

ε_r : is called the relative permittivity or dielectric constant of the medium, for vacuum $\varepsilon_r=1$, so

$$D = \varepsilon_0 E \quad \dots(2-10)$$

By substitute equation (2-10) in (2-9) we get [68,69]:

$$P = \varepsilon_0 \varepsilon_r E - \varepsilon_0 E$$

$$P = \varepsilon_0 (\varepsilon_r - 1) E \quad \dots(2-11)$$

2.9. Types of Polarization:

2.9.1. Electronic Polarization

Electronic polarization may be induced to one degree or another in all atoms. It results from a displacement of the center of the negatively charged electron cloud relative to the positive nucleus of an atom by the electric field. This polarization type is found in all dielectric materials and, of course, exists only while an electric field is present. as shown figure (2-2a).

2.9.2 Ionic Polarization

Ionic polarization occurs only in materials that are ionic. An applied field acts to displace cations in one direction and anions in the opposite direction, which gives rise to a net dipole moment. As shown figure (2-2b).

2.9.3 Orientation Polarization

The third type, orientation polarization, is found only in substances that possess permanent dipole moments. Polarization results from a rotation of the permanent moments into the direction of the applied field. This alignment

tendency is counteracted by the thermal vibrations of the atoms, such that polarization decreases with increasing temperature. as shown figure (2-2c) [70].

2.9.4 Interfacial Polarization.

The final type of polarization is space-charge polarization, sometimes called interfacial polarization, and results from the accumulation of charge at structural interfaces in heterogeneous materials. Such polarization occurs when one of the phases has a much higher resistivity than the other, and it is found in a variety of ceramic materials, especially at elevated temperatures [71,72].

Other polarizations that based on the chemical composition of the material and its components and its called (Interfacial or space charge polarization), that occurs at frequencies of low little and very under audio waves, depending on the type of defects and heterogeneity that causes the polarization [73]. as shown figure (2-2d).

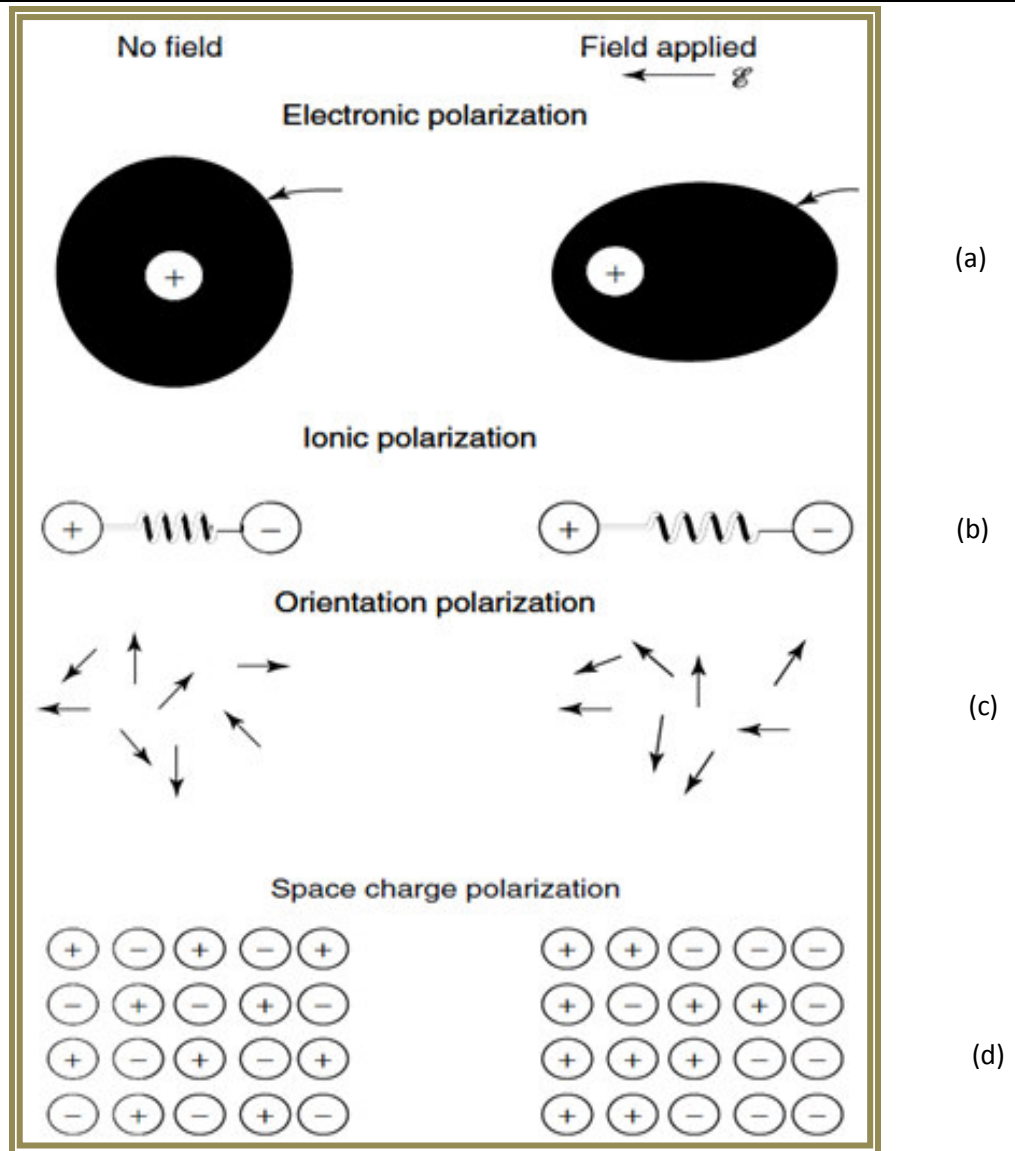


Fig. (2-2) Schematic diagram for the types of polarization. [71]

- a) *Electronic Polarization*
- b) *Ionic Polarization*
- c) *Orientation Polarization*
- d) *Space charge Polarization*

2.10. Dielectric Properties:

The outstanding feature for insulator materials in the field of electricity is the dielectric properties. Though there are many properties of dielectrics, yet the following are important from the subject of view:

1-Dielectric Constant.

2-Dielectric Loss.

3- Dielectric strength

2.10.1. Dielectric Constant

The permittivity means the charge storing capacity of a material. Consider two metal parallel plates of area (A) separated by a distance (d), in vacuum, attaching these plates to an electric circuit, the capacitance (C_o) of the parallel plates given by:

$$C_o = \frac{\epsilon_o A}{d} \quad \dots(2-12)$$

If a dielectric material is inserted between the capacitor plates, the capacitance (C) of the parallel plates will increase, as following:

$$C = \frac{\epsilon A}{d} \quad \dots(2-13)$$

Where:

ϵ : is the permittivity of the dielectric material.

The relative permittivity, (dielectric constant), of a material (ϵ_r) defined as:

$$\epsilon_r = \frac{\epsilon}{\epsilon_0} \quad \dots(2-14)$$

Since (ϵ) is always greater than (ϵ_0), the minimum value for (ϵ_r) is (1). By substitute equs. (2-14 in 2-13), the capacitance of the metal plates separated by the dielectric is :

$$C = \epsilon_r \frac{\epsilon_0 A}{d} \quad \dots(2-15)$$

$$C = \epsilon_r C_0 \quad \dots(2-16)$$

Thus (ϵ_r) is a dimensionless parameter that compares the charge-storing capacity of a material to that of vacuum. Dielectric constant depends upon the frequency of the applied electric field. It decreases with the increase in frequency. Dielectric constant also depends upon temperature[70,62,74].

2. 10.2 Dielectric loss

When an electric fields acts on any matter the latter dissipates a certain quantity of electric energy that transforms into heat energy. This is known as "loss" of power, i.e., the dissipation of an average electric power in matter during a certain interval of time. If a metal conductor is first connected to direct voltage and then to alternating voltage, the acting magnitude of which is equal to direct voltage, the loss of power (P_w in watt) in the conductor will be the same in both cases in conformity with the Joule-law and equal to [62,75]:

$$P_w = V^2/R \quad \dots(2-17)$$

Where (V) is the voltage in volt and (R) is the resistance of the conductor in ohms. As distinct from conductors, most of the dielectrics display a characteristic feature, under a given voltage the dissipation of power in these dielectrics depends on the voltage frequency.

The expense of power at an alternating voltage is markedly higher than at a direct voltage, and rapidly grows with an increase in frequency, voltage, and capacitance, and also depends on the materials of the dielectric.

A dielectric loss is an amount of power loss in an electrical insulator. Dielectric losses at a direct voltage can easily be found from eqn. (2-17) where (R) stands for the resistance of the insulator, while the losses under an alternating voltage are determined by more intricate regularities. When considering dielectric losses we usually mean the losses precisely under an alternating voltage. Let the alternating voltage ($V=V_0\exp(j\omega t)$) be applied to a circuit containing a capacitor, with air as a dielectric medium. The current (I) passing through the capacitor according to Ohm's law.

$$I = \frac{V}{X_c} \quad \dots(2-18)$$

Where (X_c) is the impedance of the capacitor of a capacitance (C)

$$X_c = \frac{1}{Cj\omega} \quad \dots(2-19)$$

Considering the dielectric material in a capacitor (c), $\omega=2\pi f$, where, ω is the angular frequency f is the frequency

$$j = \sqrt{-1}$$

The current (I) may be calculated by substitute equation (2-17) in (2-19) and the result in equation (2-20) as follow:

$$I = j\omega\varepsilon_r C_o V \quad \dots(2 - 20)$$

The current (I) in a dielectric is (90°) advanced in phase in relation to the voltage as shown in figure (2-3), this implies that we have a capacitive component of the current, then the heat for the system equal to zero, thus the energy is transferred in a dielectric without losses and emission of heat "Ideal dielectric".

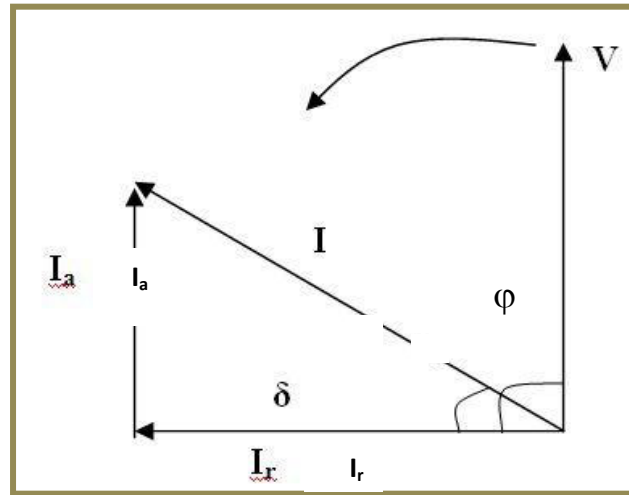


Fig. (2-3) Simplified diagram of currents in a loss dielectric.[62]

In actual fact the phase angle (φ) is slightly less than (90°), the total current (I) through the capacitor can be resolved into two components active (resistive current) (I_a) and reactive (capacitive current) (I_r) currents [76].

The phase angle is very close to (90°) in a capacitor with a high quality dielectric, the angle (δ) is a more descriptive parameter which, when added to the angle (φ), brings the angle (φ) to (90°).

$$\delta = 90^\circ - \varphi \quad \dots(2 - 21)$$

The angle (δ) is the dielectric loss angle. If (δ) is small, therefore ($\sin\delta \approx \tan\delta$). The tangent of this angle is equal to the ratio between the active and reactive currents:

$$\tan \delta = \frac{I_a}{I_r} \quad \dots(2-22)$$

$\tan\delta$ is the dielectric loss tangent or dissipation factor. It is important to note that the dielectric response of a solid can be succinctly described by expressing the relative dielectric constant as a complex quantity,

$$\varepsilon_r = \varepsilon_r' - j\varepsilon_r'' \quad \dots(2-23)$$

In which ε_r' is the real component of dielectric constant of the material, and (ε_r'') is the imaginary component, is known as the dielectric loss factor [77,78].

We can find the value of (I_a) and (I_r) by substituting equ. (2-23) in equ. (2-20):

$$I = j\omega(\varepsilon_r' - j\varepsilon_r'')C_o V \quad \dots(2-24)$$

$$I = \omega\varepsilon_r'' C_o V + j\omega\varepsilon_r' C_o V \quad \dots(2-25)$$

The total current (I) in terms of the components (I_a) and (I_r) are:

$$I = I_a + jI_r \quad \dots(2-26)$$

$$I_a = \omega\varepsilon_r'' C_o V \quad \dots(2-27)$$

$$I_r = \omega\varepsilon_r' C_o V \quad \dots(2-28)$$

By substituting equations (2-27) and (2-28) in eqn. (2-22) we can get

$$\tan \delta = \frac{\varepsilon_r''}{\varepsilon_r'} \quad \dots(2-29)$$

The quality factor (Q) of an insulator portion is determined, the reciprocal value of the loss tangent [79]:

$$Q = 1/\tan\delta = \cot\delta \quad \dots(2-30)$$

The expression form for the value of dielectric losses (P_w) in an insulation portion having a capacitance (c) [80]:

$$P_w = VI_a = VI_r \tan\delta \quad \dots(2-31)$$

2.10.2.1. dielectrics Temperature Dependent

Effects of temperature on the dielectric properties of ceramics were carried out up to a maximum temperature. It was observed that the dielectric constant of ceramic material increases with increase of temperature. In dielectrics, ionic polarization increases the dielectric constant with increase in temperature [81]. An electron interacts through its electrical charge with the ions or atoms of the lattice and creates a local deformation of the lattice. The deformation tends to follow the electron as it moves through the lattice. The combination of the electron and its strain field is known as polaron. The atoms or molecules in the samples cannot in most cases orient themselves at low temperature region. When temperature rises the orientation of dipoles is facilitated and small polaron motion may result from the absorption of one or more phonons and this process is essentially the hopping mechanism. The contribution from the conventional band mobility and from hopping mechanism are additive. ceramic materials like semiconductors, their resistivity decreases with increase in temperature and show arrhenius type temperature dependence according to the equation[81]:

$$\rho = \rho_0 \exp (E_a /kT) \quad \dots\dots\dots (2-32)$$

where, (E_a) in equation(2-32), is thus called the activation energy of hopping and the graph between ($\ln \rho$) and ($1/T$) is linear in some cases but usually a curve is

also observed. (E_a) values are found to be in the range of (0.1-0.5) eV. But at very high temperatures the chaotic thermal oscillations of molecules are intensified and the degree of orderliness of their orientation is diminished thus the permittivity passes through a maximum value.

The materials having the higher resistivity at room temperature have associated high activation energy. Many workers have established the relation between resistivity and the stoichiometry. The presence of excess iron leads to the formation of more ions, so in the preparation of high resistivity ceramics, it is necessary to avoid excess iron in the lattice by adding cobalt and manganese which inhibit the formation of ions.

2.10.2.2. Frequency dependent

At low frequencies, e.g. audio frequencies (10^3 Hz) May contribute to each of the four polarizations (α_e) is electronic polarizability, (α_i) ionic polarizability, (α_d) dipolar polarizability and (α_s) space charge polarizability) in the composition of total polarization (α). In this case, when a dielectric material is subjected to an alternating field the orientation of dipoles and hence the polarization will tend to reverse every time the polarity of the field changes. As long as the frequency remains low ($< 10^6$ Hz) the polarization follow the alternations of the field without any significant lag, while at radio frequencies the dipole will no longer be able to rotate sufficiently rapidly so that their oscillation will begin to lag behind those of the field. At microwave frequencies ($\sim 10^9$ Hz) the permanent dipoles, if present in the medium, will be completely unable to follow the field and the contribution to the orientation polarization would be increased . The time scale of ionic polarizations is such that they do not occur at frequencies higher than infrared ($\sim 10^{12}$ Hz). This leaves the electronic polarization which is observable into the (UV) but is relaxed out at (X-ray) frequencies [82]. In good dielectric materials, the limiting low frequency permittivity is composed of only ionic and electronic polarizability. A general

relation of the following form explains the variation of dielectric constant with frequency[82].

$$\varepsilon'' = (\sigma - \sigma') / \varepsilon' \omega \quad \dots\dots\dots (2-33)$$

where (ε') and (ε'') are the real and imaginary part of dielectric constant, (σ) and (σ') are the (d.c) and (a.c) conductivities respectively, and (ω) is the angular frequency which is equal to ($2\pi f$). The imaginary part of permittivity describes the energy loss from an (AC) signal as it passes through the dielectric material. The real part of relative permittivity is also called dielectric constant, and which explains the relationship of the (AC) signal's transmission speed and the dielectric material's capacitance. Dissipation factor (tangent loss) is the ratio of the energy dissipated to the energy stored in the dielectric material.

2.10.3 Dielectric Strength

The average potential per unit thickness at which failure of the dielectric material occurs [83]. Whichever, the magnitude of the electric field required to cause dielectric breakdown is called the dielectric strength [71,84]. When applied to a strong electric field on the insulator is higher than the value of the specific critical, the relatively high electrical current will apply, So the insulation properties of the insulator will lose and become a conductor [85]. The voltage that occurs then the breakdown is called (Breakdown Voltage). When divided by the thickness of the samples [86]. As equation following [58,87]:

$$\text{Dielectric strength} = \frac{\text{breakdown voltage}}{\text{insulator thickness}}$$

$$E_{br} = \frac{U_{br}}{h} \quad \dots\dots\dots (2-34)$$

$$U_{br} = E_{br} \cdot h$$

Where:

E_{br} : Dielectric strength, and calculated by units: (kV/mm) or (V/ μ m) [83].

U_{br} : break down voltage, h : dielectric thickness.

When very high electric fields are applied across dielectric materials, large numbers of electrons may suddenly be excited to energies within the conduction band. as a result, the current through the dielectric by the motion of these electrons increases dramatically, sometimes localized melting, burning, or vaporization produces irreversible degradation and perhaps even failure of the material [70,89]. Typical dielectric strengths of polymers are in the range of (20-50)kV/mm, which are approximately (2-10) times higher than ceramics and glasses and are hundreds of times higher than conducting metals and alloys. The dielectric strength for oxide ceramic insulators lies in the range (1-20) kV/mm, with the value of (9) kV/mm for Al_2O_3 being typical [71] and dielectric Strength can be reduced by Cracks, impurities and pores [86].

A breakdown can be seen in the material by watching one of the following cases: -

1. Hole in the sample, which occurs when reach the real electrical durability of the insulation.
2. Burn or melt, which occurs when the material is heated locally and breakdown, occurs [90].

It is important to notice that the dielectric strength of dielectrics vary depending on where in the applying-voltage (d.c) give (25-30)% values higher than the voltage (a.c) at the frequency (60Hz) [91], as in NaCl, where the value of E_{br} (3.8×10^4 kV/cm) in the (d.c) while the (1.4×10^3 kV/cm) in the (a.c), and this difference can be attributed to the loss of relaxation [92]. When alternating voltage is applied on insulator, there are several phenomena that occur in the insulator from electrical conduction and polarization, as the lead increased voltages on the insulator to increase the flow of leakage current and capacitance current for alternating voltage, and upon the arrival of voltage to the greatest value, which represents the state of the breakdown of the insulator it is in this

moment pass conduction current is within the insulator and increasingly after the voltage of decreasing due to reduced resistance to insulator, and this situation often represent a circle between the source poles. The breakdown of solid insulators describe all stages of isolation, where a crash of the material, the phenomenon consists of the speed rise of the current for voltage above a certain value, can be described graphically the relationship between the current and the voltage in three regions. as in figure (2-4) :

The first: In the region (I): - The relationship to Ohm's law with a high current linearly with increasing voltage until it reaches to the values not exceeding micro amper.

The second: In the region (II): - saturation region where the current remains constant despite increasing voltages.

The third: In region (III): - an increase in current is increasingly voltages above a certain value, which is breakdown voltage (U_{br}) [92].

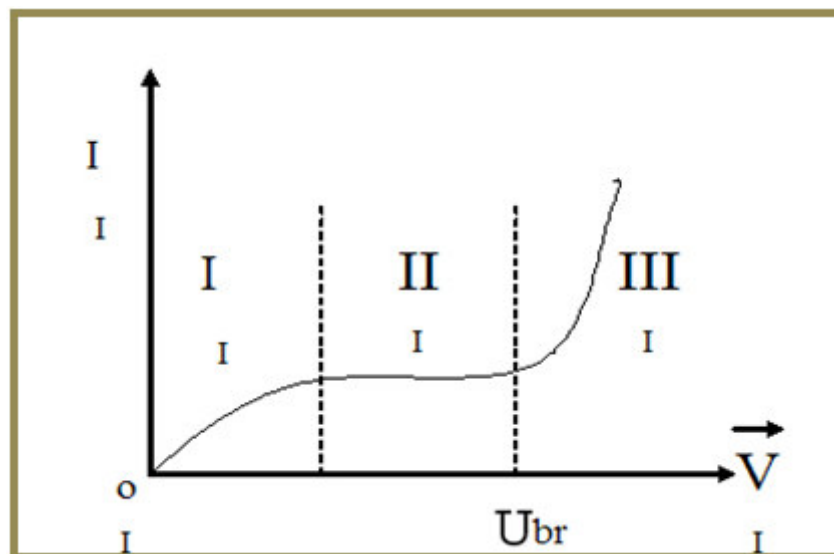


Fig. (2-4) Shows the relationship between Current and Voltage In The Solid Insulators. [92]

The mechanism of failure and the breakdown strength changes with the time of voltage application and for discussion purposes it is convenient to divide the time scale of voltage application into regions in which different mechanisms operate [93]. As shown in figure (2-5)

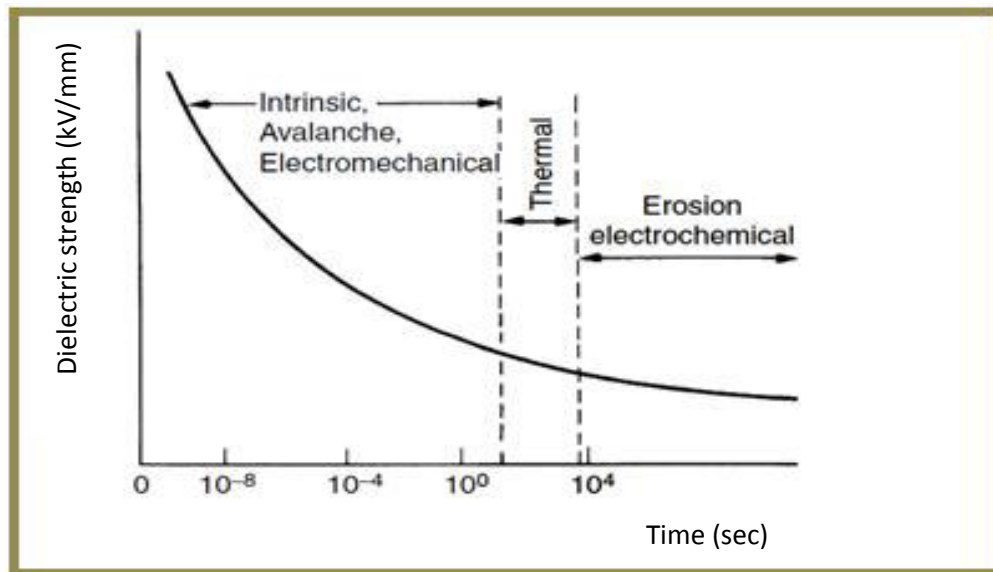


Fig. (2-5) Mechanisms of Failure and Variation of Breakdown Strength in Solids with Time of Stressing.[93]

2.11. The Main Types of Breakdown that occur In dielectrics

2.11.1 Intrinsic Breakdown:

Correlate defines of The Intrinsic Breakdown to solid materials by pure material characteristics, and empty of defects under test circumstances that lead to break down at maximum voltage. The real Intrinsic Breakdown that cannot get it by experiences but the measures at low temperature and applying voltage (d.c) to short periods .it can reach to pure value [94].

This type of breakdown has to do with the presence of free electrons is a noticeable phenomenon in alkali halides, mica, glass and others. It occurs under room temperature [92]. Increasing electric intensity of the solid material rapidly under the influence of voltages very short period to the maximum that is called **(Intrinsic Electric Strength)** and get this value practically under the best circumstances the process when removed externalities where the value depends on the type of material and the temperature only [95].

Characterized by self-breakdown of the following advantages:

1. Short time of increasing voltage up sometimes to microseconds (10^{-8} - 10^{-7}) sec and the breakdown occurs at once after applying the voltage then the so-called pure breakdown.
2. The little dependence to dielectric strength and breakdown voltage with a frequency voltages and this property is necessary to compare the values of the peak voltage affecting whether a pulses or sine wave voltage.
3. If the influence of the regular electric field on insulator, the dependence of the dielectric strength on the insulator material dimensions and its pole, is a little bit [62].
4. Little dependence of the dielectric strength on the temperature [96].

2.11.2 Electrothermal Breakdown

The presence of the electric field produces a voltage applying on insulation material heat. Therefore dielectric loss continues more. Electrothermal breakdown develops as follows: voltage applied to the insulation material produces heat, which leads to raising the temperature of insulation material and the loss continues even further. The most accurate theory of the Electrothermal breakdown developed by the two Soviet researchers (Fok and Semenov). According to this theory, the breakdown voltage of the homogeneous insulator layer in a state of Electrothermal breakdown (under alternating voltage) will be equal to [62]:

$$U_{br} = 382 \sqrt{\frac{\lambda}{f \varepsilon_i \alpha \tan \delta_i}} \varphi(\beta h) \quad (2-35)$$

Where:

U_{br} : Breakdown Voltage, (kV).

λ : Coefficient of Thermal Conductivity, (W/(m.K)).

f : Voltage frequency, (Hz).

ε_i, δ_i : Permittivity and loss angle at initial temperature before applying voltage on the insulator .

α : Thermal coefficient of dielectric losses factor, (K^{-1}).

h : Thickness of the dielectric, (m).

β : Coefficient of describes retrieval the heat from insulator to the environment.

Where[62]:

$$\beta = \frac{\lambda_1 Q}{2\lambda(\lambda_1 + Qh_1)} m^{-1} \quad (2-36)$$

λ_1 : Coefficient of thermal conductivity of the poles material.

Q : Coefficient of thermal conductivity from poles to the environment ($W/(m^2.K)$).

h_1 : Thickness of Pole, (mm).

When the dimensions of (βh) high and increasing, the function ($\varphi(\beta h)$) can be equal to (0.662) approximately. In the case if the poles is very thin, we assume ($h_1 = 0$) in equation (2-36) and which can get a simplified expression for the limit (β)[62]:

$$\beta = \frac{Q}{2\lambda} m^{-1} \quad (2-37)$$

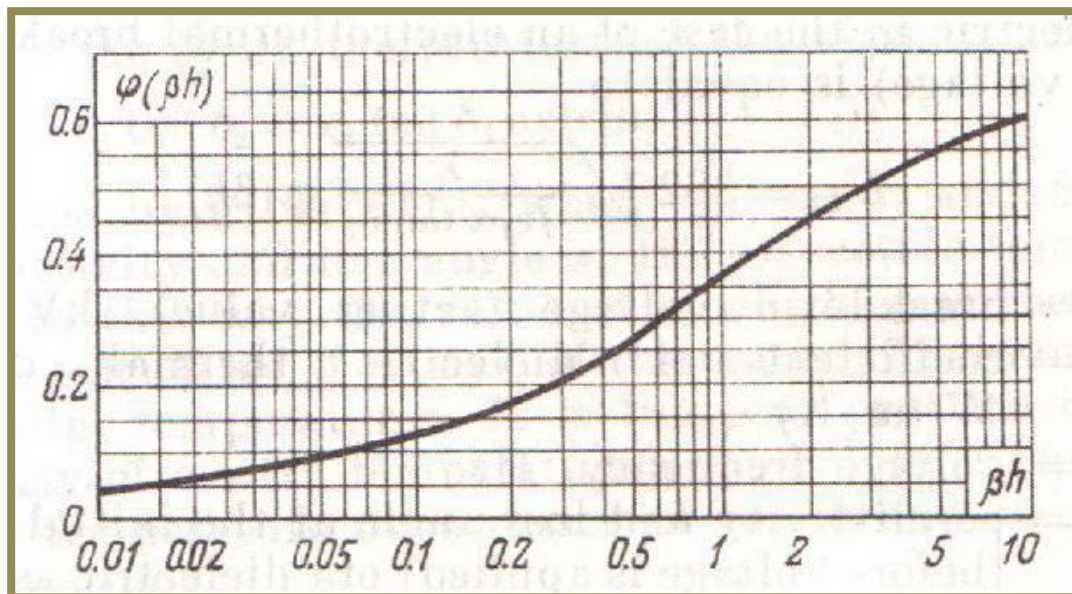


Fig. (2-6) draw to function ($\varphi(\beta h)$), and the (x-axis) logarithmic. [62]

As follows from equations (2-28) and (2-29) for the thickness of the dielectric layer is very large ($h_1 = \infty$), there must be ($\beta h = \infty$) and ($\varphi(\beta h) = 0.662$), so U_{br} when ($h_1 = \infty$), is gaining a maximum specific value:

$$U_{br} = 253 \sqrt{\frac{\lambda}{f \varepsilon_i \alpha \tan \delta_i}} \quad kV \quad (2-38)$$

In the state of Electothermal breakdown, the dielectric strength of the materials can guess its dependence on:

1. Voltage frequency, dielectric strength decreased with frequency increased.
2. The temperature, dielectric strength decreased with temperature increased.
3. The time during the application of voltage [62,93].

When applying electric field to the dielectric at room temperature, so the conduction current is in general very little, but its value increases rapidly with the temperature of the crystal. The heat generated from the current conduction will arrive partially to the environment and absorbed in partially to raise the temperature of the crystal which in turn will increase the average generated heat. If the average of heat generation at any point in the insulator exceeds the rate of heat lost to the outside, produces then non-stabilizing and can be the sample of submission to the thermal breakdown [97,98].

There are several factors affecting on the thermal breakdown voltage of the ceramics like geometrical structure, size (especially thickness), thermal conductivity, specific heat of ceramic, environment heat (ambient), the rate of increase in voltage, the value of the ($\tan \delta$) and change its with temperature, and relative dielectric constant [94].

2.11.3 Electromechanical Breakdown:

During the test dielectric breakdown, the poles that touched surface of the sample will shed exert forces on the sample surface by Coulomb's attractive mutual of the poles (**Coulomb attraction of the electrodes**).

Substances which can deform appreciably without fracture may collapse when the electrostatic compression forces on the test specimen exceed its mechanical compressive strength. The compression forces arise from the electrostatic attraction between surface charges which appear when the voltage is applied. The pressure exerted when the field reaches about (10^6 V/cm) may be several kN/m^2 . Following Stark and Garton, if (d_0) is the initial thickness of a specimen of material of Young's modulus (Y), which decreases to a thickness of d (m) under an applied voltage (V), then the electrically developed compressive stress is in equilibrium with the mechanical compressive strength if [93]:

$$\epsilon_0 \epsilon_r \frac{V^2}{2d^2} = Y \ln\left(\frac{d_0}{d}\right) \quad (2-39)$$

or:

$$V^2 = \frac{2Y d^2}{\epsilon_0 \epsilon_r} \ln\left(\frac{d_0}{d}\right)$$

Where (ϵ_0) and (ϵ_r) are the permittivity of free space and the relative permittivity of the dielectric.

Differentiating with respect to (d) we find that expression (2-32) has a maximum when $[d/d_0 = \exp[-1/2]] = 0.6$. Therefore, no real value of (V) can produce a stable value of (d/d_0) less than (0.6). If the intrinsic strength is not reached at this value, a further increase in (V) makes the thickness unstable and the specimen collapses. The highest apparent strength is then given by:

$$E_a = \frac{V_c}{d_0} = \frac{d}{d_0} E_a \approx 0.6 \left(\frac{Y}{\epsilon_0 \epsilon_r} \right)^{1/2} \quad (2-40)$$

This treatment ignores the possibility of instability occurring in the lower average field because of stress concentration at irregularities, the dependence of Y on time and stress, and also on plastic flow [95].

2.11.4 Streamer Breakdown

Under certain controlled conditions in strictly uniform fields with the electrodes embedded in the specimen, breakdown may be accomplished after the passage of a single avalanche. An electron entering the conduction band of the dielectric at the cathode will drift towards the anode under the influence of the field gaining energy between collisions and losing it on collisions. On occasions the free path may be long enough for the energy gain to exceed the lattice ionization energy and an additional electron is produced on collision. The process is repeated and may lead to the formation of an electron avalanche similar to gases [93].

Figure (2-7) is shown a cross-section of a simplified example represents testing of a dielectric slab between sphere-plane electrodes. Ignoring the field distribution, i.e. assuming a homogeneous field .

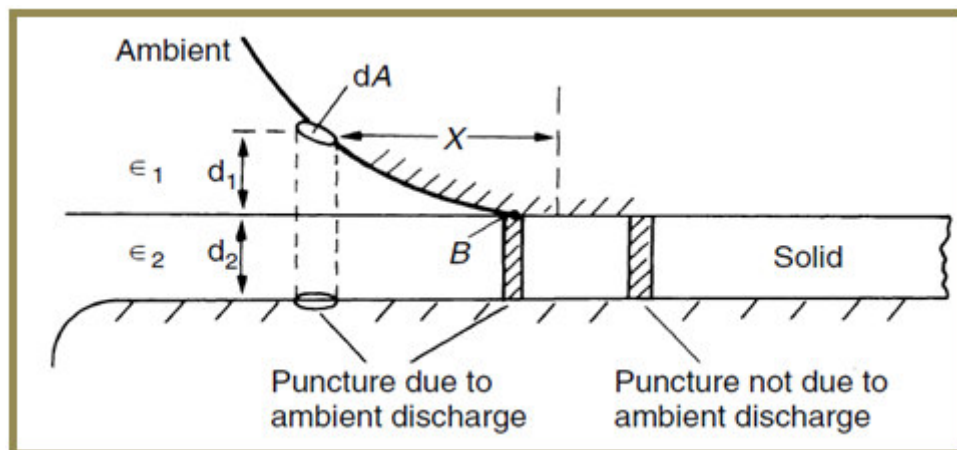


Fig. (2-7) Breakdown of Solid Specimen due to Ambient Discharge-Edge Effect.[93]

If we consider an elementary cylindrical volume of end area (dA) spanning the electrodes at distance (x), then on applying the voltage (V)

between the electrodes, a fraction (V_1) of the voltage appears across the ambient given by:

$$V_1 = \frac{V d_1}{d_1 + \left(\frac{\epsilon_1}{\epsilon_2}\right) d_2} \quad (2-41)$$

here (d_1) and (d_2) represent the thickness of the media (1) and (2) in figure (2-7) and (ϵ_1) and (ϵ_2) are their respective permittivities. For the simple case when a gaseous dielectric is in series with a solid dielectric stressed between two parallel plate electrodes, the stress in the gaseous part will exceed that of the solid by the ratio of permittivities. For the case shown in, the stress in the gaseous part increases further as distance (x) is decreased, and reaches very high values as (d_1) becomes very small (point B). Consequently the ambient breaks down at a relatively low applied voltage. The charge at the tip of the discharge will further disturb the applied local field and transform the arrangement to a highly non-uniform system. The charge concentration at the tip of a discharge channel has been estimated to be sufficient to give a local field of the order of (10 MV/cm), which is higher than the intrinsic breakdown field. A local breakdown at the tips of the discharge is likely, therefore, and complete breakdown is the result of many such breakdown channels formed in the solid and extending step by step through the whole thickness. The breakdown event in solids in general is not accomplished through the formation of a single discharge channel, but assumes a tree-like structure as shown in figure (2-8) which can be readily demonstrated in a laboratory by applying an impulse voltage between point-plane electrodes with the point embedded in a transparent solid, e.g. (plexiglass). The tree pattern shown in figure (2-8) was recorded by Cooper with a (1/30 μ sec) impulse voltage of the same amplitude. After application of each impulse the channels were observed with a microscope and new channels were recorded. Not every impulse will produce a channel. The time required for this type of breakdown under alternating voltage will vary from a few seconds to a few minutes. The tree-like pattern discharge is not limited specifically to the

edge effect but may be observed in other dielectric failure mechanisms in which non uniform field stresses predominate [93,98,99].

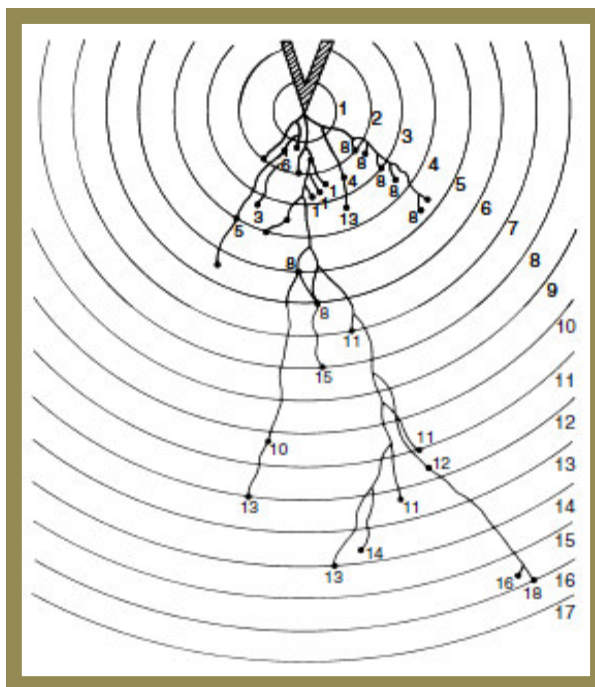


Fig. (2-8) Breakdown channels in plexiglass between point-plane electrodes.[93]

2.10.5 Erosion Breakdown

Practical insulation systems often contain cavities or voids within the dielectric material or on boundaries between the solid and the electrodes. These cavities are usually filled with a medium (gas or liquid) of lower breakdown strength than the solid. Moreover, the permittivity of the filling medium is frequently lower than that of the solid insulation, which causes the field intensity in the cavity to be higher than in the dielectric. Accordingly, under normal working stress of the insulation system the voltage across the cavity may exceed the breakdown value and may initiate breakdown in the void [93]. lately, informations level about Erosion breakdown exposed from researchers Mason and Kreuger [97,98]. Figure (2-9) shows a cross section of a dielectric of thickness (d) containing a cavity in the form of a disc of thickness (t) together with an analogue circuit. In the analogue circuit the capacitance (C_c) corresponds to the cavity, (C_b) corresponds to the capacitance of the dielectric

which is in series with (C_c), and(C_a) is the capacitance of the rest of the dielectric.

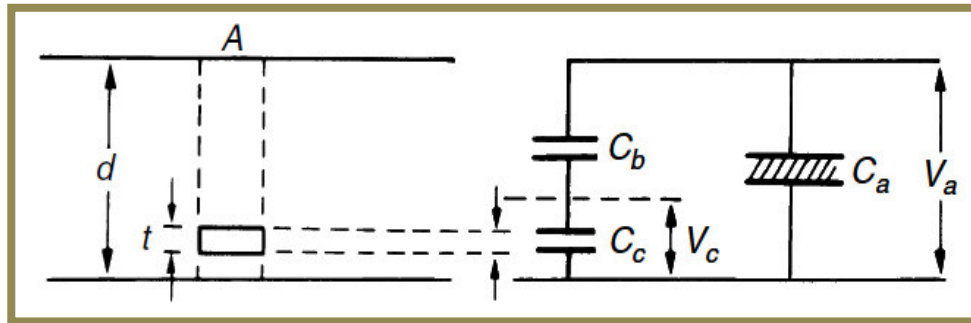


Fig. (2-9) Electrical discharge in cavity and its equivalent circuit.[93]

For ($t \ll d$), which is usually the case, and assuming that the cavity is filled with gas, The voltage across the cavity is:

$$V_c = V_a \epsilon_r \frac{t}{d} \dots\dots\dots (2 - 42)$$

Where (ϵ_r) is the relative permittivity of the dielectric.

Under an applied voltage (V_a) when (V_c) reaches breakdown value (V^+) of the gap (t) , the cavity may break down. The sequence of breakdowns under sinusoidal alternating voltage is illustrated in figure (2-10) The dotted curve shows qualitatively the voltage that would appear across the cavity if it did not break down. As (V_c) reaches the value (V^+), a discharge takes place, the voltage (V_c) collapses and the gap extinguishes. The voltage across the cavity then starts increasing again until it reaches (V^+), when a new discharge occurs. Thus several discharges may take place during the rising part of the applied voltage. Similarly, on decreasing the applied voltage the cavity discharges as the voltage across it reaches (V^-). In this way groups of discharges originate from a single cavity and give rise to positive and negative current pulses on raising and decreasing the voltage respectively [93]. When the gas in the cavity breaks down, the surfaces of the insulation provide instantaneous cathode and anode. Some of the electrons impinging upon the anode are sufficiently energetic to

break the chemical bonds of the insulation surface. similarly, bombardment of the cathode by positive ions may cause damage by increasing the surface temperature and produce local thermal instability. Also channels and pits are formed which elongate through the insulation by the 'edge mechanism'. Additional chemical degradation may result from active discharge products, e.g. (O_3) or (NO_2), formed in air which may cause deterioration. Whatever is the deterioration mechanism operating, the net effect is a slow erosion of the material and a consequent reduction of the breakdown strength of the solid insulation [93,97-99].

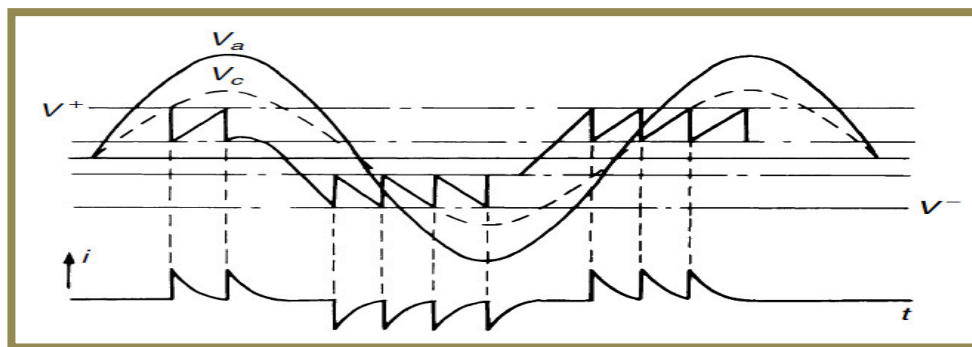


Fig. (2-10) Sequence of cavity breakdown under alternating voltages.[93]

2.12. Factors Affecting on the Dielectric Strength

We cannot describe the breakdown mechanism within a fixed factor that change with it ,because the testing requirements will change during the measurement, where the factors are interrelated and influence on each another. [62,92].

We will expose these factors as follows:

1- Internal Structure of the dielectric

Where the dielectric strength depends on internal structure of the dielectric in terms of homogeneity and purity, as the presence of defects such as dislocations or interacted crystals as possible to cause the electrical connect paths, as well as the electrons that found because impurity atoms or excited heat gives the energy due to the applying field and these produce (electrons) due to atomic electronic collisions. If any of the electrons got enough energy to create a

pair (electron - hole) by electron collision of an electron, after that the extra electrons will collide and break by similar manner and breakdown happened [85].

2- Engineering and the Type of Poles

The poles between the source of high voltage and the dielectric effect on the dielectric strength, where increasing the area of the poles (in comparison to the dimensions of the dielectric) reduces the break voltage and that the increasing points of the penetrating of the dielectric and the possibility of a break in the weakest of those points, as well as affect the geometry and the type of poles in the possibility of a burn or melt or crack in the dielectric [62,92].

3- Humidity

Effect of humidity on the dielectric strength of dielectrics, where dielectric strength decreasing when the amount of humidity content increased, the influence of humidity increases with increasing temperature [62,94].

4- Frequency

The losses in alternating fields are much higher than the continuous fields, because the loss in the relaxation phenomenon such as the movement of dipole depends on the rate of change of field, and as a result of this the intensity of electrothermal breakdown be less of alternating fields and decrease by the source voltage frequency increase [99]. It is mention that the intrinsic breakdown doesn't depend as much as on frequency, while electrothermal breakdown depend greatly on frequency [62,92].

5- Thickness of dielectric

The dielectric strength changing with a thickness of dielectric is not linear, but decrease to an increase of thickness, that prefer to measure the dielectric strength when thickness be little to estimate the value of breakdown accurately, and can explain why the decrease to the difficulty of heat recovery and taking out from the insulator to the environment, leading to increase dielectric loss and decreased dielectric strength. Also, the increase in thickness

reduces the electric field generated by the applying voltage [62,95]. As shown in figure (2-11)

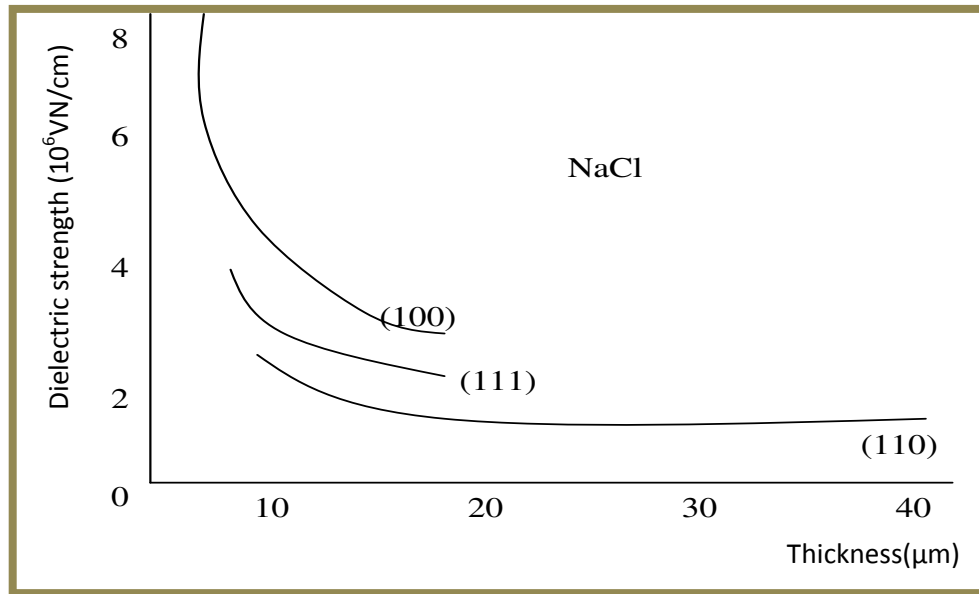


Fig. (2-11) Effect of thickness on the dielectric strength. [92]

6-Temperature

Influence of temperature on the electrical breakdown where it's in intrinsic breakdown affect on the interaction of an electron–phonon, At low temperatures ($T \ll 25^\circ\text{C}$) the phonon interactions are weak, so that the electrons gain more energy in the electric field and be able to generate many of the free electrons, and breakdown voltage be relatively low. The breakdown voltage at room temperature taken maximum values where the phonon interactions are important but less than under room temperature as long as the thermal vibration can generate new electrons and the intrinsic breakdown strength less dependent on temperature. The electrothermal breakdown is most common in the ceramic insulators the influence of the temperature effect is clear as the reasons for the breakdown can be attributed to the temperature of the environment or loss of connectivity, which generate heat at a faster rate than the rate of disposal and removal, this leads to increased local heat. In general, the dielectric strength decreases with increasing temperature as shown in figure (2-12)[92,94,100].

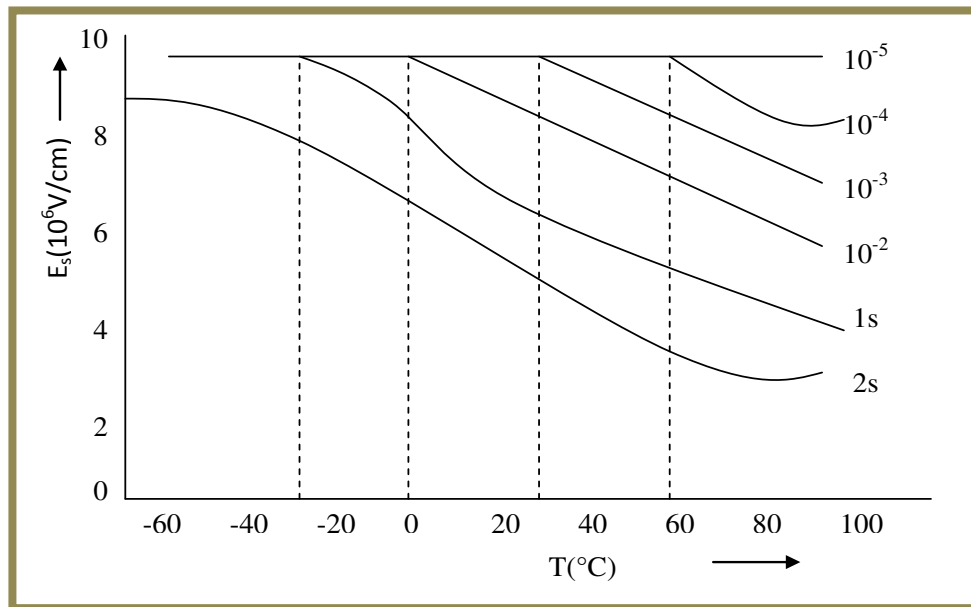


Fig. (2-12) Effect of temperature on dielectric strength.

7- Voltage Elevating Average

The voltage elevating average is a function of the dielectric strength in solid materials, where the voltage elevating average determines type of breakdown, where the range $(10^{-8}-1)$ sec is the extent of intrinsic breakdown, while the range $(0.1-10^3)$ min is the extent of electrothermal breakdown. Where applying voltage more time increases the possibility of occurring a electrothermal breakdown. Since the behavior of electrothermal breakdown associated with the time rate of rise of voltage, which can lead to local heat to the material as the loss of electrical power over time leads to raise the temperature more and more local connectivity, in addition to this, voltage elevating average possible cause cumulative effects of the collision (chemical and electrochemical) and corrosion, which in turn destroy the material and speeds up the breakdown by heating. Also, the increase in voltage elevating average leads to reduce the time required for two collisions consecutive for the same electron, leading to speed in a process of ionization and thus the speed of the breakdown, the lack of stability and evaporation that occurs due to the increase localized in temperature leads to the passage of high currents, which in turn lead to hole dielectric. It was found that voltage elevating average and

temperature effect on the behavior of breakdown of some ceramics, where depends on the conductivity characteristics and structure. Accordingly, in the medium temperature based on voltage elevating average [76,92,94,101]. There are several from affecting factors on dielectric strength such as the time during voltage applying, samples environment, method of applying field (d.c, a.c, pulses.....etc.), samples ageing, mechanical stress, porosity...etc. [62,102,103].

Chapter Three



Experimental Part

3.1 Introduction

This chapter shows the experimental part and the process of preparation of nano (Al_2O_3) with testing methods such as (XRD, SEM) and studying electrical and physical properties.

3.2 Raw materials

1- Aluminium nitrate nonahydrate $\text{Al}(\text{NO}_3)_3 \cdot 9\text{H}_2\text{O}$ with purity of (99%) from Riedel-Dehaen company / Germany

2- urea with purity (99%) from Fluka company

3- Distilled water

3.3 Tools and equipment

Volumetric flasks , filter paper , beakers , magnetic stirrer ,Oven , furnace , then for testing XRD , SEM , Archimedes basis ,Vickers hardness , LCR Meter and dielectric strength instrument were used, .

3.4 Preparation of alumina by (sol-gel method)

1-Solution preparation

$\text{Al}(\text{NO}_3)_3 \cdot 9\text{H}_2\text{O}$ (35gm) was dissolved in (35 ml) of deionized water at (22°C) in a beaker and then placed on a magnetic stirrer . Urea (72gm) was added to the solution.

2- Filtration process

The solution was filtered to remove any insoluble impurities .

3-Heating process

The solution was heated at (100°C) for (12hrs) to produce transparent gel

4- Drying process

The gel of alumina was heated at (280°C) for (1hrs) to produce a yellow powder.

5- Washing and filtration processes

The powder washed several times with distilled water and then filtered .

6- Drying process

Drying the powder was done at (70°C) for (2hrs) to produce a white color powder

7- Molding equipment

There are many types of equipment used in powder compacting. These are the molds. A mold is designed for the manufacture of samples in the form of pellet in diameter (1cm) and thickness (5mm) . It uses hydraulic press with a pressure of (500-700) psi, and the diameter of the mold used (1cm) with a height of (3cm).

8. Heating process

The pellet sample of alumina was heated at (350°C) to study the change of properties with temperature .

3.5 Instrument

3.5 .1 X – ray diffraction

X-ray diffraction is one of the most important characterization tools used in solid state chemistry and materials science . XRD is an easy tool to determine the size and the shape of the unit cell for any compound. Powder diffraction methods is useful for qualitative analysis (phase Identification), quantitative analysis (Lattice parameter determination and Phase fraction analysis) etc. Diffraction pattern gives information on translational symmetry – size and shape

of the unit cell from peak positions and information on electron density inside the unit cell , namely where the atoms are located at peak intensities .It also gives information on deviations from a perfect particle , if size is less than roughly (100 nm) , extended defects and micro strain from peak shapes and widths .

Testing of X-ray diffraction of the oxides prepared by using a diffraction X-ray type (XRD-6000) with an accelerating voltage of (220/50)HZ , of the SHIMADZU company (JAPAN) that generates (1.5406Å) to the source of the target (Cu) and within range of angular ($2\theta = 20^\circ - 60^\circ$) which is shown in the fig. (3-1).



Fig. (3-1) XRD instrument used

3.5.2 Scanning electron microscope (SEM)

The scanning electron microscope (SEM) uses a focused beam of high-energy electrons to generate a variety of signals at the surface of solid specimens. The signals that derive from electron sample interactions reveal information about the sample including external morphology (texture), chemical composition, and crystalline structure and orientation of materials making up the sample. In most applications, data are collected over a selected area of the surface of the sample, and a 2-dimensional image is generated that displays spatial variations in these properties. Areas ranging from approximately (1 cm) to (5 microns) in width can be imaged in a scanning mode using conventional SEM techniques (magnification ranging from 20X to approximately 30,000X, spatial resolution of 50 to 100 nm) . The SEM is also capable of performing analyses of selected point locations on the sample, this approach is especially useful in qualitatively or semi-quantitatively determining chemical compositions [104] . The scanning electron microscope used in imaging the nanoparticles is a VEGA//EasyProbe which is a favorable combination of a scanning electron microscope and a fully integrated energy dispersive X-ray microanalyser produced by TESCAN, s.r.o., Libušina trída 21 SEM . vega 3 from Belgium .

3.6 physical properties

A – Density

B – Porosity and water absorption

3.6.1 Density

The density of alumina was measured by (Archimedes Basis) by measure the dry weight of pellets by sensitive balance and put it in water in container and leaved it for (24 hour) , the soaked pellets weight was measured and then measure the weight of sample when it suspended inside the water and the equation below was applied to calculate the density and as the figure (3-2) .

$$\text{Density} = (W_D) \text{gm} / (W_s - W_I) \text{gm} \dots \dots \dots (3-1)$$

3.6.2 Porosity and water absorption

The porosity was measured by measuring the (dry weight) of pellet with sensitive balance and then a pellet was inserted in water for (24 hrs) to measure the (soaked weight) and then the (suspended weight) measured and apply the relation below to calculate the apparent porosity and as the figure (3-2) .

$$\% \text{ AP} = (W_s - W_D) \text{gm} \times 100 / (W_s - W_I) \text{gm} \dots \dots (3-2)$$

$$\text{WA}\% = (W_s - W_D / W_D) \times 100\% \dots \dots \dots (3-3)$$



Figure (3-2) Archimedes Basis

3.7. Mechanical test (Hardness)

Vickers hardness test is used to measure the hardness of samples , it inserts a tool sutures (indenter) in several regions of the surface of the sample . Hardness test a very small diamond indenter having pyramidal geometry is forced into the surface of the specimen . The angle between the faceted (136°) are calculated through the Vickers hardness as follows:

$$V.H = \frac{F}{d^2/2 \sin \frac{1}{2}(136^\circ)} \dots\dots\dots(3-4)$$

$$V.H = 1.854 \frac{F}{d^2} \dots\dots\dots(3-5)$$

Where :

F : Represents the load hanging,

D : Represents the average impact of diameter.

3.8. Electrical properties

LCR meter is used to measure the resistance, capacitance, inductance, impedance, loss factor etc. of the materials. In an automatic LCR meter bridge method, the bridge circuit employs a fixed standard resistor beside the unknown Impedance and a multiplying digital to analog convertor (MDAC) that works as a resistive potentiometer. The type of LCR meter is Agilent impedance analyzer an American origin, its range of frequency (50Hz-5MHz), as in the figure (3-3)

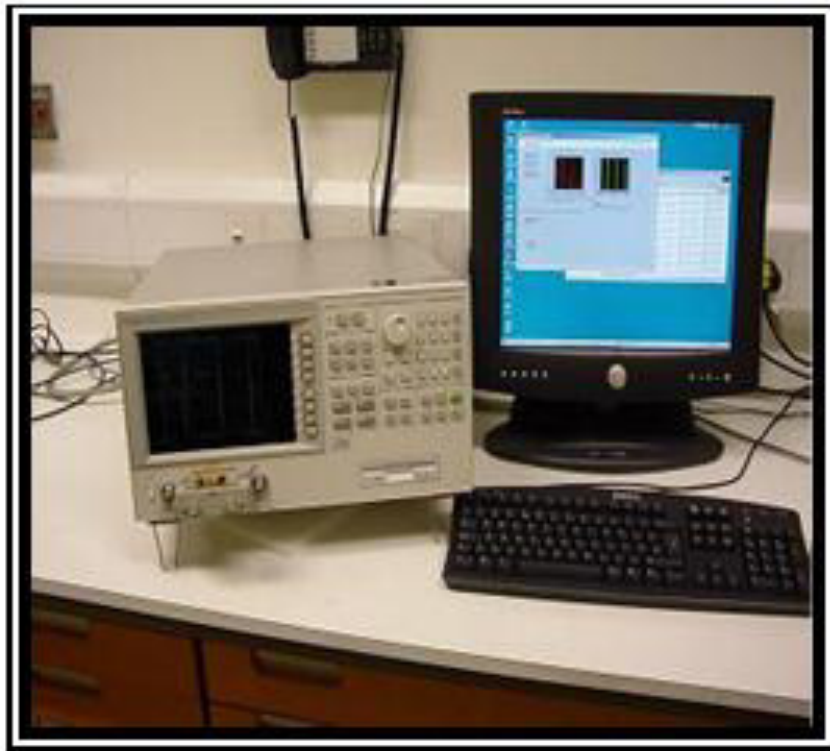


Fig. (3-3) LCR Meter

3.8.1 Electrical resistivity

The electrical resistivity was measured by computerized LCR meter, the sample was put between the poles and make sure that the poles touch sample surface. Electrical resistivity data have been recorded on computer's screen via mathematic formulas studied previously eq(2-4) .

3.8.2 Electrical conductivity

The electrical conductivity was measured by computerized LCR meter, the sample was put between the poles and make sure that the poles touch sample surface. Electrical conductivity data have been recorded on computer's screen via mathematic formulas studied previously eq(2-4)

3.8.3 Dielectric Constant

The dielectric constant was measured by computerized LCR meter, the sample was put between the poles and make sure that the poles touch sample surface. Dielectric constant data have been recorded on computer's screen via mathematic formulas studied previously eq(2-14).

3.8.4 Dispersion Factor (Tangent Loss)

The Tangent Loss was measured by computerized LCR meter , the sample was put between the poles and make sure that the poles touch sample surface. Dispersion factor data have been recorded on computer's screen via mathematic formulas studied previously .

3.8.5 Dielectric Strength

The sample was put between two copper poles which are embedded in oil to make sure of touching poles and sample surface and to overcome the transfer of flashover then applying voltage through the sample and that see the breakdown voltage. After knowing the area that breakdown happens which can be distinguish according to the damage that occur because of the breakdown and as the figure (3-6) .

$$E_{br} = U_{br} / h \dots \dots \dots (3-6)$$



Fig. (3-4) Dielectric strength instrument

Chapter Four



**Results
and
Discussion**

4-1 Introduction

This chapter includes the results and discussions, study of the (X-ray diffraction, scanning electron microscope (SEM), density, porosity, hardness, dielectric constant, electrical conductivity, electrical resistivity , tangent loss and breakdown voltage)

4-2 Structures Test

4-2-1 XRD pattern of (Al₂O₃) powder

The results of X-ray diffraction show that the material prepared at (280°C) is gamma-alumina after comparison with international alumina card (JCPDS) files No.(46. 1215) where the matching with the peaks (100) , (112) , (113) observed from the test it appears that the main stream of crystallization is toward (113). The selecting range of temperature (280°-350°)C was after preparing of some samples at a temperature less than (280°C) , which gives non-completely reaction , also the samples prepared at a temperature more than (350°C) results in undesirable materials . The XRD of alumina prepared at (280°C) is shown in fig (4-1) .

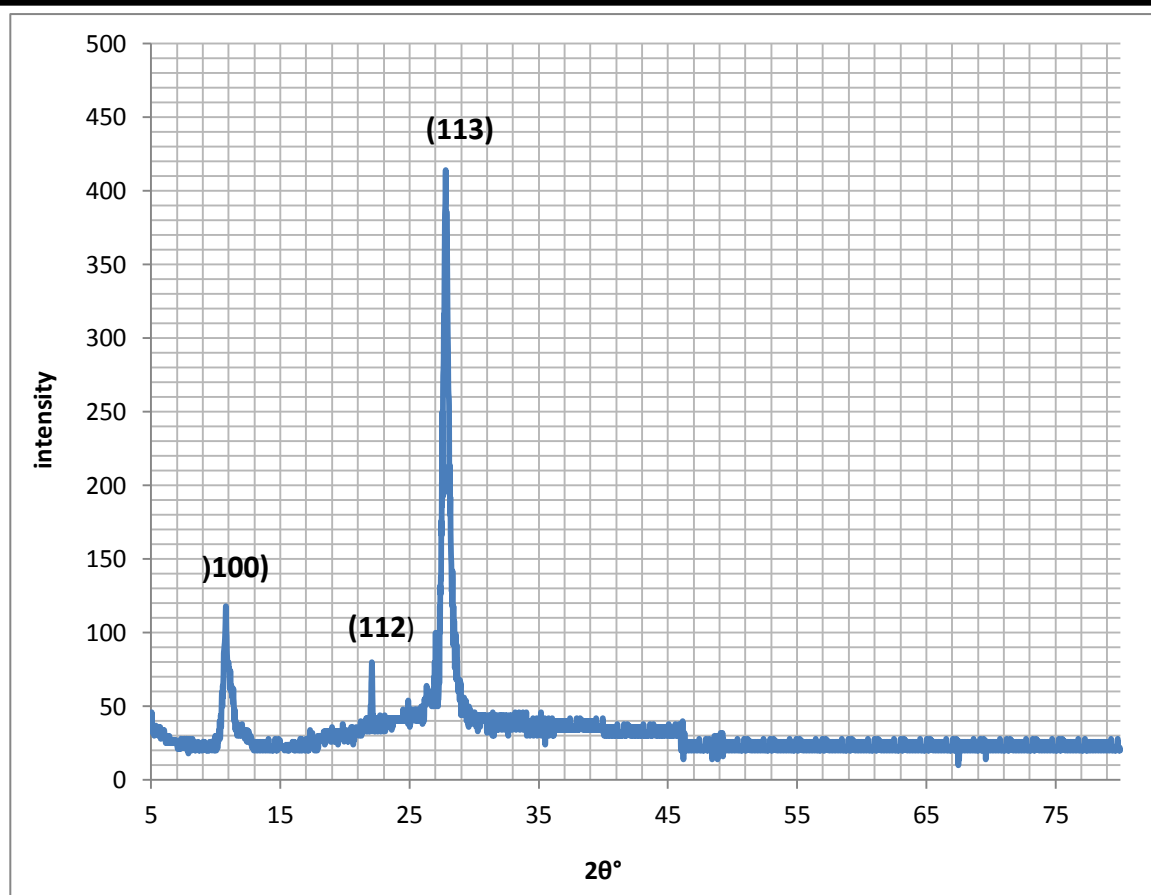


Figure (4-1) XRD patterns of Al_2O_3 prepared at $280\text{ }^\circ\text{C}$

We observed also that after heating the sample at $350\text{ }^\circ\text{C}$, the peaks be more matching with the same card (JCPDS) files No.(46. 1215) by the planes of (120) , (117) , (152), (335) , (046) , (113) , (123) ,which is defined as miller indices and this mean that the high temperature lead to rearranging the atoms and getting a good properties as in figure (4-2)

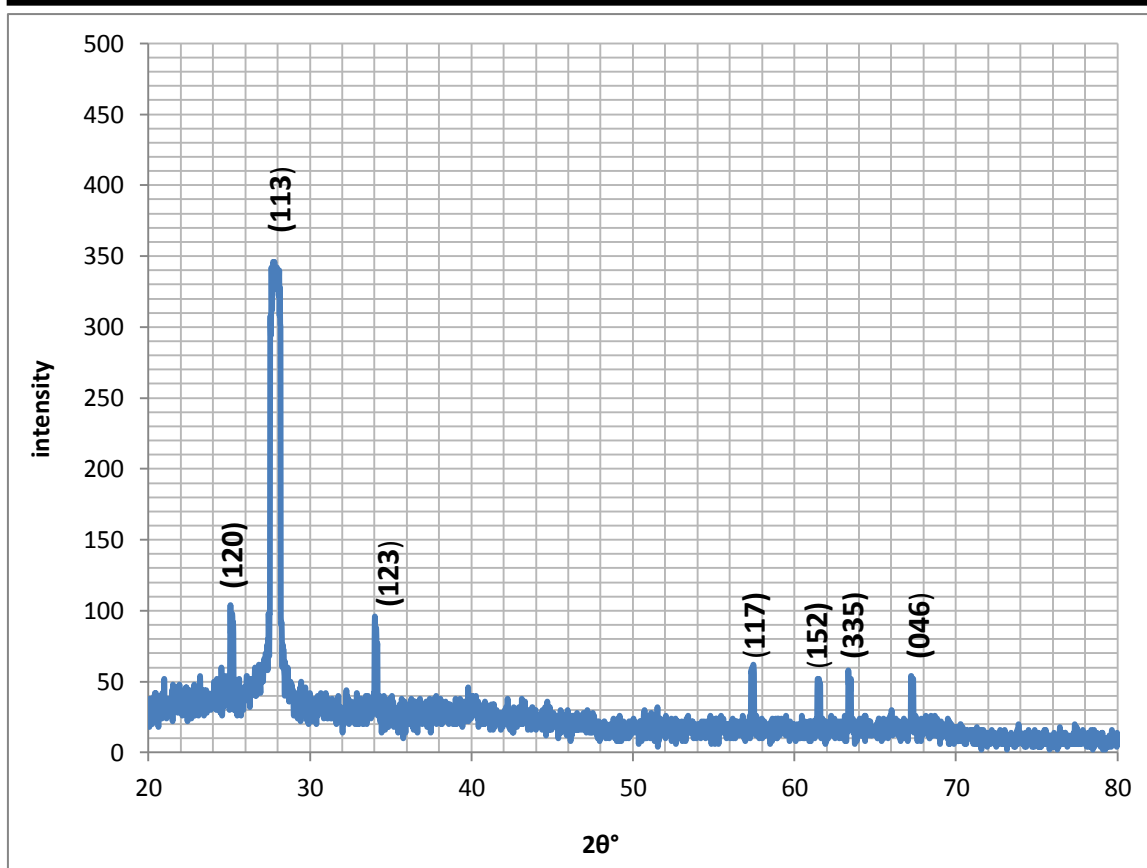


Figure (4-2) XRD patterns of Al₂O₃ prepared at 350°C

Table (4-1) the location of peaks in fig (4-1) and fig (4-2)

Sample	2 θ (degree)	hkl
Al ₂ O ₃ (JCPDS)	11.092	010
	11.092	100
	21.906	112
	25.063	120
	25.063	210
	27.148	022
	27.148	202
	27.769	113
	34.101	123
	34.101	213
	57.478	117
	57.478	226
	61.434	152
	61.660	512
	63.540	335
	67.196	046
67.251	406	
Al ₂ O ₃ at 280C°	10.924	(100),(010)
	22.087	112
	27.047	(022),(202)
	27.842	113
Al ₂ O ₃ at 350C°	25.160	(120),(210)
	27.877	113
	34.088	(123),(213)
	57.495	(117),(226)
	61.503	(152),(512)
	63.403	335
	67.292	(046),(406)

4-2-2 Particle size calculation from x-ray diffraction of Al₂O₃

From this study and by considering the peak at degrees, average particle size has been estimated by using Debye-Scherrer formula using the more intense peak .

(a) for sample prepared at (280 °C) :

$$D = 14.8 \text{ nm}$$

(b) for sample heated at (350 °C) :

$$D = 20 \text{ nm}$$

So the average particle sizes of the Al₂O₃ calcined at (280°C) and (350 °C) are about (14.8) and (20 nm) respectively, which demonstrate that the average particle sizes increased as the calcining temperature increased. During the calcining the diffusion of particle to particle followed by the formation of grain boundary and the closing of voids and neck growth proceeds rapidly but powder particles remain discrete. The structure recrystallizes and particles diffuse into each other. Isolated pores tend to become spheroidal and densification continues at a much lower rate [105] .

4-2-3 SEM of Al₂O₃ powder prepared at 280 °C

The SEM images of the Al₂O₃ sample prepared by precipitation methods and calcined at (280°C) is shown in figure (4-3).

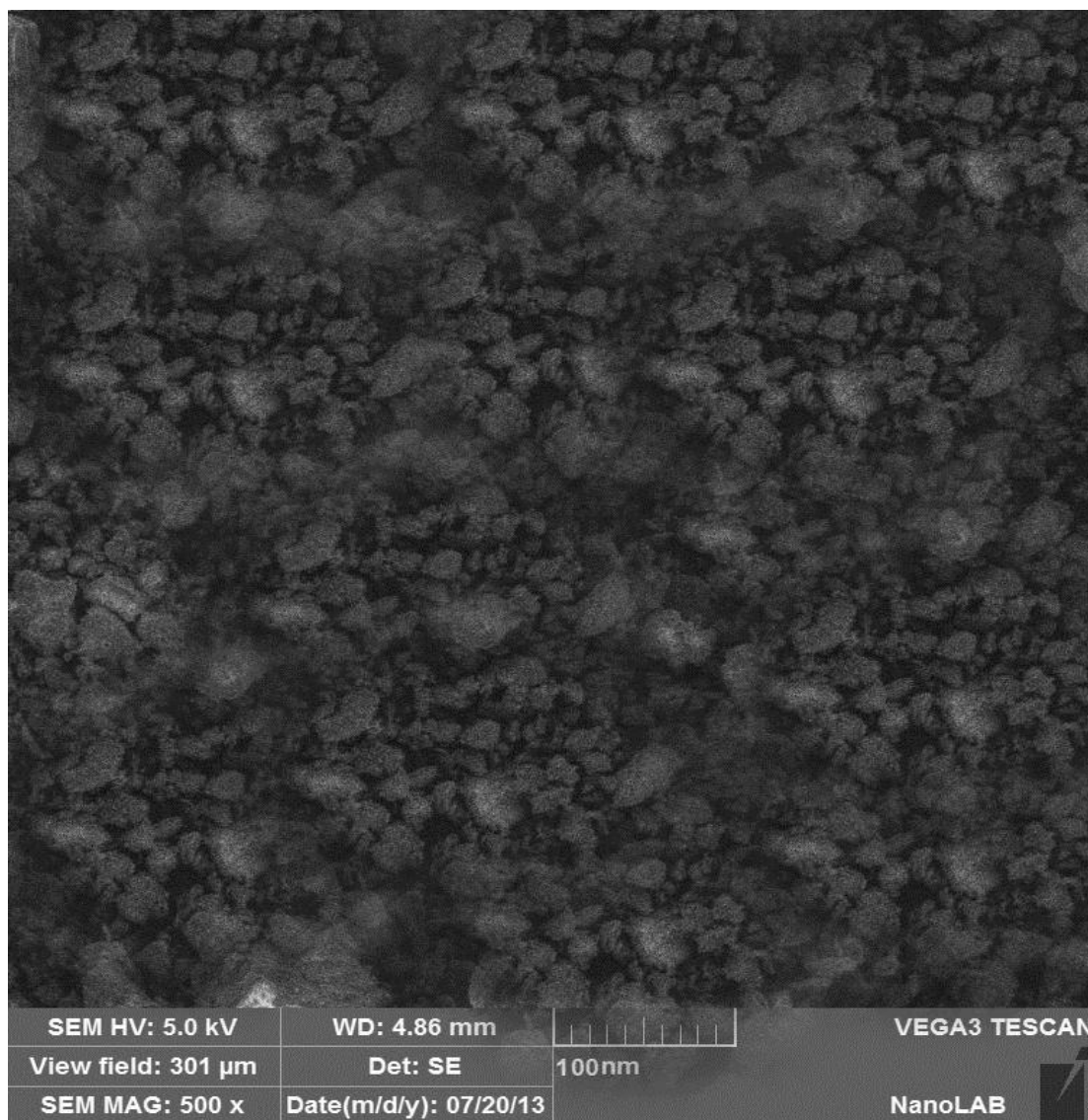


Figure (4-3) SEM images of Al₂O₃ powders prepared at (280°C)

It can be observed that the powders are composed of non-agglomerated and non-spherical particles, with the formation of soft agglomerates with irregular morphology constituting the quite fine particles. The study of SEM micrographs reveals a less number of pores with smaller lump size, also it indicates the homogeneity of the prepared alumina. But when the sample is

heated at (350°C) ,we observed increasing in grain size and decrease the porosity because of agglomeration in the sample , also it observed that the grain size which determined by SEM images as in fig (4-4) are closer to that estimated by Debye – Scherrer formula [106] .

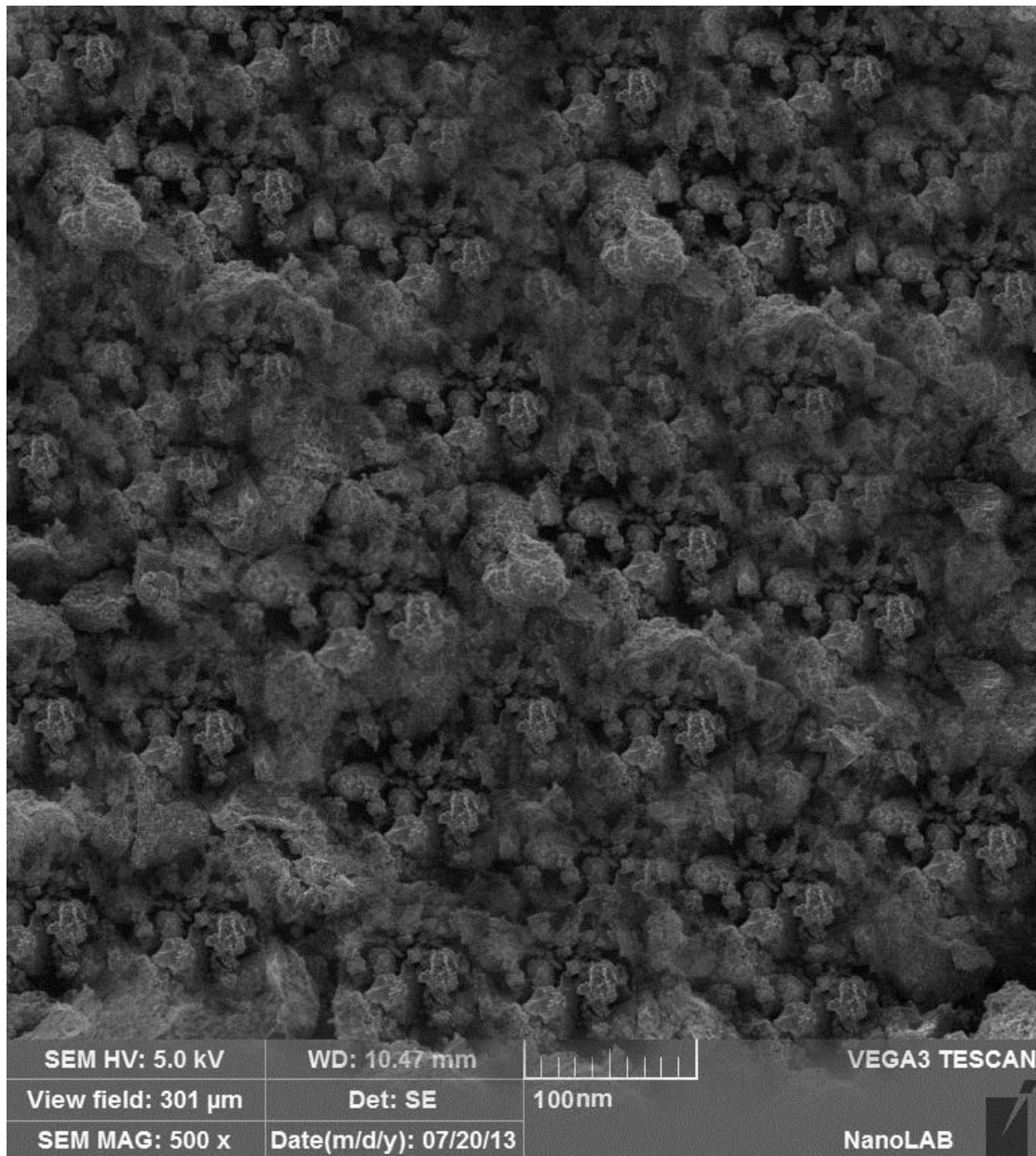


Figure (4-4) SEM images of Al₂O₃ powders prepared at (350°C)

4-3 Physical properties

4-3-1 Density test

Calculation of alumina density at different temperatures. Experimentally, density measurements are performed using Archimedes' principle. The errors associated with this method derive mainly from thermal, surface effects, pore present and specimen size. Density of the samples is measured using distilled water as fluid medium and the apparent density values are shown in table (4-2).

Table (4-2) apparent density values of alumina

Density for sample prepared at	
280°C	350°C
1.692 g/cm ³	1.841 g/cm ³

There is an increase in the density resulted from shrinkage of the pellets with an increase of temperature, but the porosity shows otherwise [48].

4-3-2 Calculation of porosity

Table (4-3) porosity of alumina

porosity for sample prepared at	
280°C	350°C
6.857	2.068

The data in table (4-3) clarify that the value of porosity varies between (6.857%) and (2.068%) which is related to the particle size. Moreover, the change in the porosity for all investigated samples is might be the difference in the melting point of the oxides used, i.e. the melting point of Al₂O₃ (280 °C) is lower than that of Al₂O₃ (350 °C). The difference in temperature used for each method also lead to a change in the number of pores also the changes which is

happened in the contiguous grain of powder after heating and contain changing in the shape of pores this lead to increase the size of grain also decrease the rate of pores and growth in the grain [48] .

4-4 Mechanical test (Hardness)

which is a measure of a material resistance to localized plastic deformation (a small dent or a scratch). Early hardness tests are based on natural minerals with a scale constructed on the ability of one material to scratch another that is softer. Vickers hardness (V.H) is used to measure the hardness of samples [49]. The hardness of alumina is shown in table (4-4)

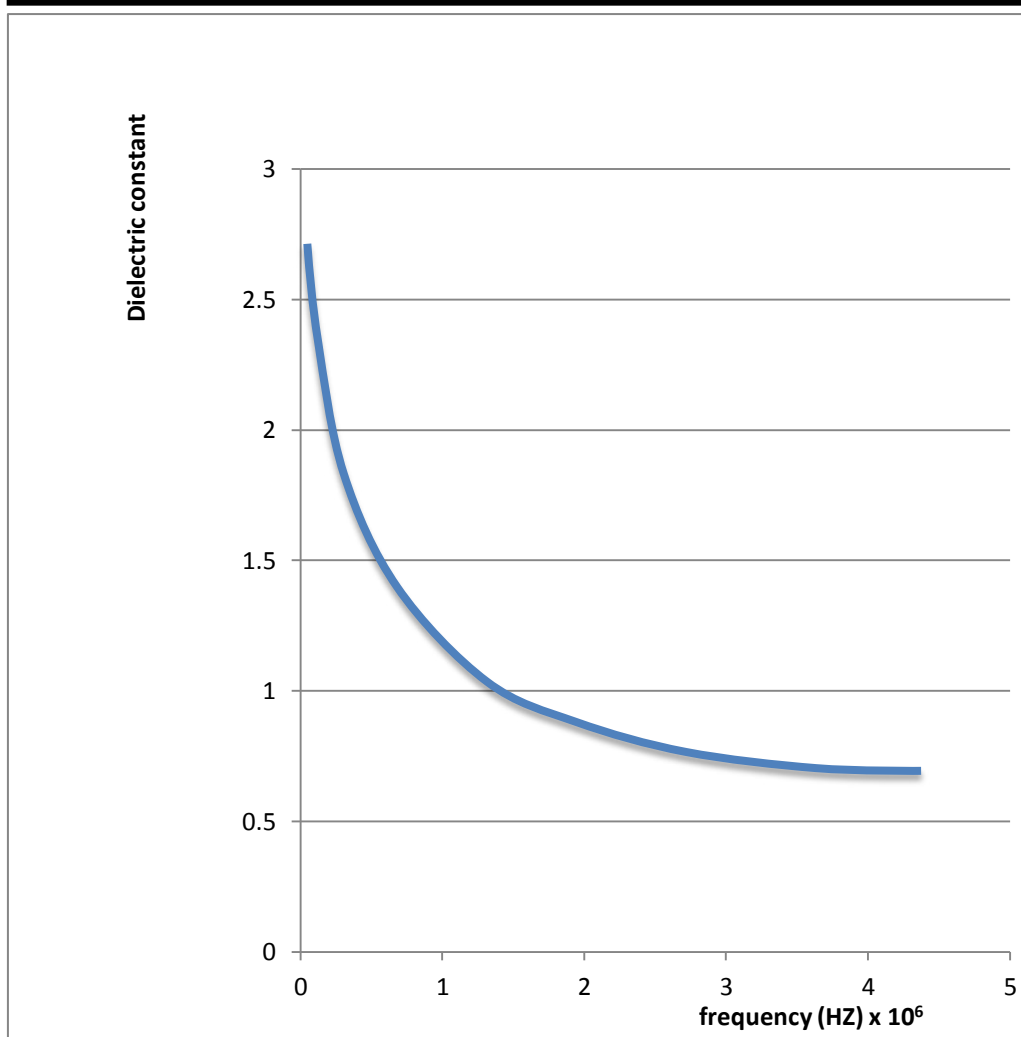
Table (4-4) Vickers hardness test of Al_2O_3 prepared at 280°C and 350°C

Sample	<i>V. H</i> Al_2O_3 at 280°C	<i>V. H</i> Al_2O_3 at 350°C
alumina	18 GPa	22 GPa

4.5. Electrical properties of alumina

4.5.1. The dielectric constant of alumina prepared at (280°C) and (350°C)

The dielectric constant have been computed for different frequencies in the range of (50 Hz to 5×10^6 Hz) it is high at low frequencies and it decrease rapidly with increasing of frequency as shown in the figure (4-5) for sample at (280°C) .



Figure(4-5) dielectric constant dependent on frequency applied for sample calcined at (280 C°)

A high value of dielectric constant is observed at lower frequencies which later falls down rapidly with frequency increase. This behavior can be explained on the basis that at lower frequencies there exist four different types of polarization (i.e. electronic, ionic, dipolar and space charge) contributions take a part in the dielectric constant, but at higher frequencies some of polarization contributions relax out, result in the lowering of dielectric constant .

But when we burn the sample at (350°C) it observed that the dielectric constant is decrease with increasing of temperature because of getting grain growth which lead to decrease in the grain boundaries and this lead to decrease

the electrical resistivity and this lead also to decrease in the dielectric constant as shown in the figure(4-6) .

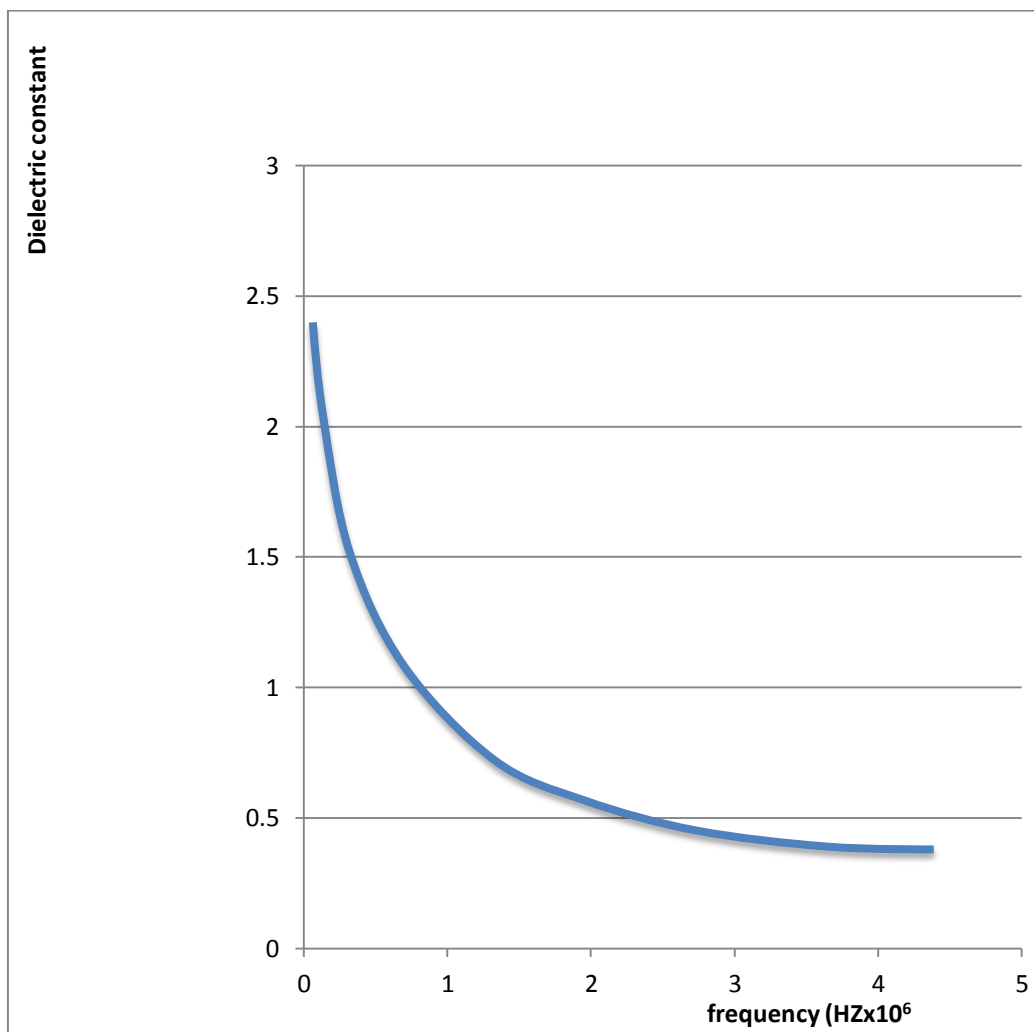


Fig (4-6) dielectric constant dependent on frequency applied sample calcined at (350 C°)

The effect of interfacial polarization decreases as a result of the decrease in porosity of the sample heated to (350 C°) , as the porosity value causes increase in dielectric constant and tangent loss as shown in table (4-3) which explain the decrease of porosity with temperature increasing [81] .

4.5.2. Dielectric losses

The dielectric loss tangent ($\tan \delta$) have been computed for different frequencies in the range of (50 Hz to 5×10^6 Hz) and it is observed to be decrease with increase in the frequency of the applied AC field. As in figure (4-7) for sample at (280 C°), The values of tangent loss ($\tan \delta$) are high at low frequencies and low at high frequencies. At higher frequencies, where the resistivity is small and the grains are more effective in electrical conductivity, a small amount of energy is required for the electrons to be exchanged between ions located in the grains and thus the energy losses ($\tan \delta$ or ϵ'') are also low [62].

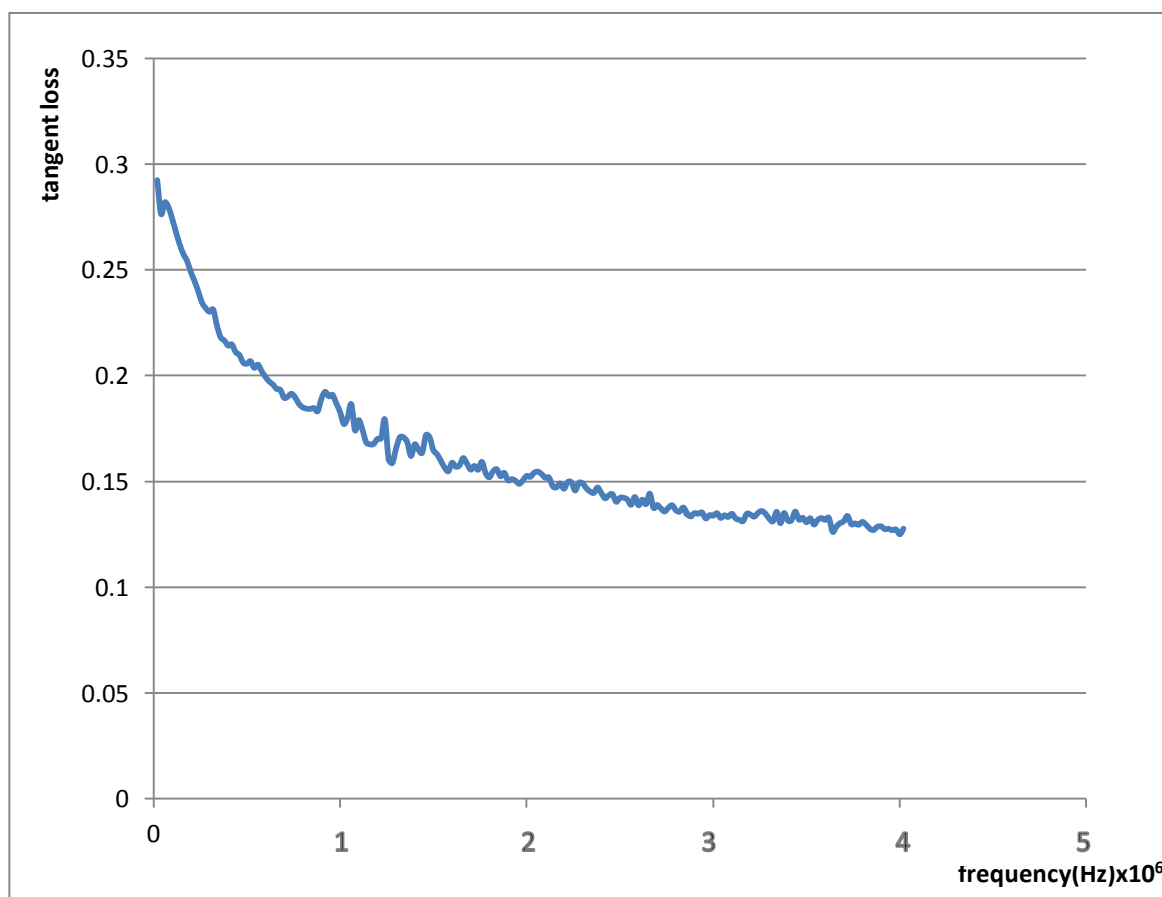


Figure (4-7): the variation of tangent loses with frequency for sample calcined at (280 C°)

But when we heat the sample at (350°C) the tangent loss is decrease more than at (280°C) this mean that the increase of temperature and frequency lead to decrease in tangent loss as in figure (4-8) [62,75] .

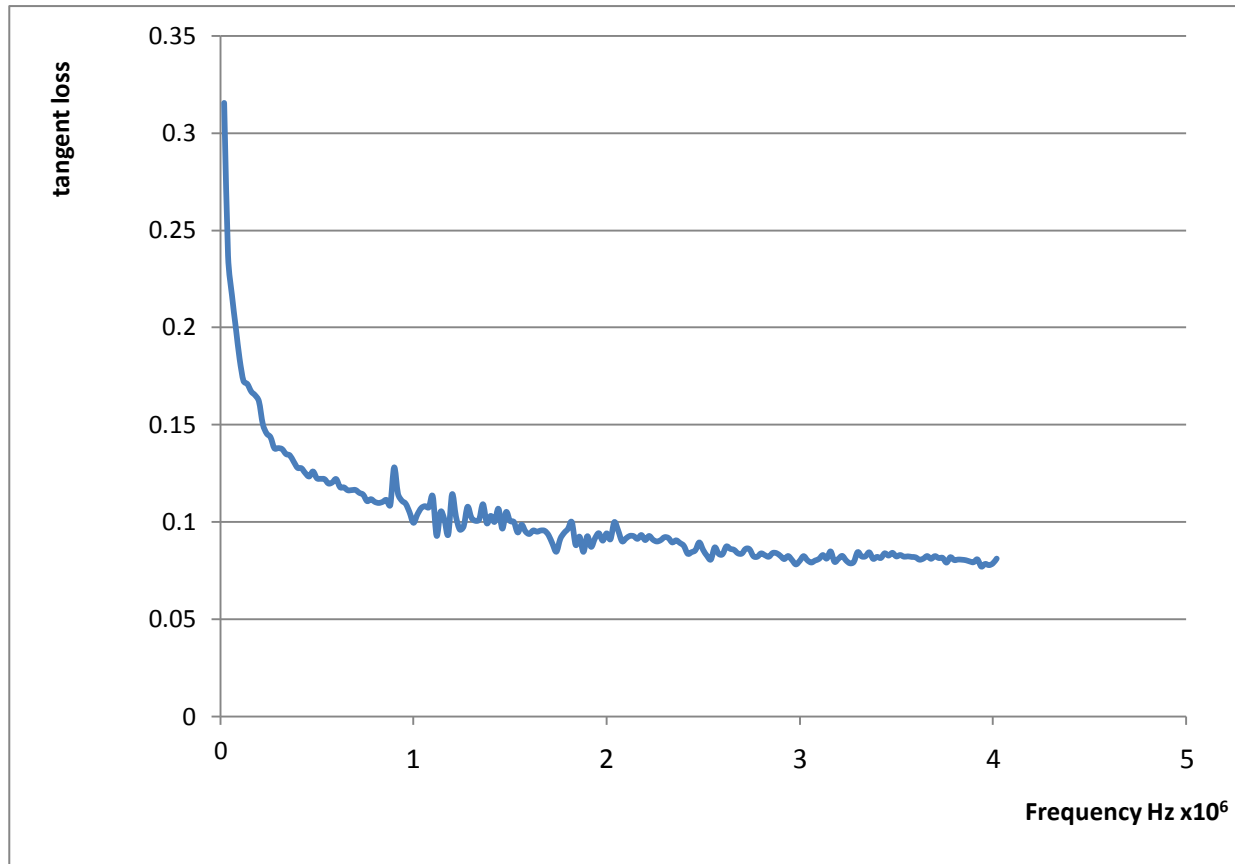


Figure (4-8): the variation of tangent losses with frequency at (350°C)

4.5.3. Electrical conductivity

The electrical conductivity (σ) of the samples was determined using LCR meter. The electrical conductivity has been computed for different frequencies in the range of (50 Hz to 5×10^6 Hz) at different temperatures. It was observed that the electrical conductivity increases with increase in frequency and this is because of increase in mobility of electron and this leads to increase of electrical conductivity. This variation is the same for all samples as in figure (4-9) for the first sample at (280°C).

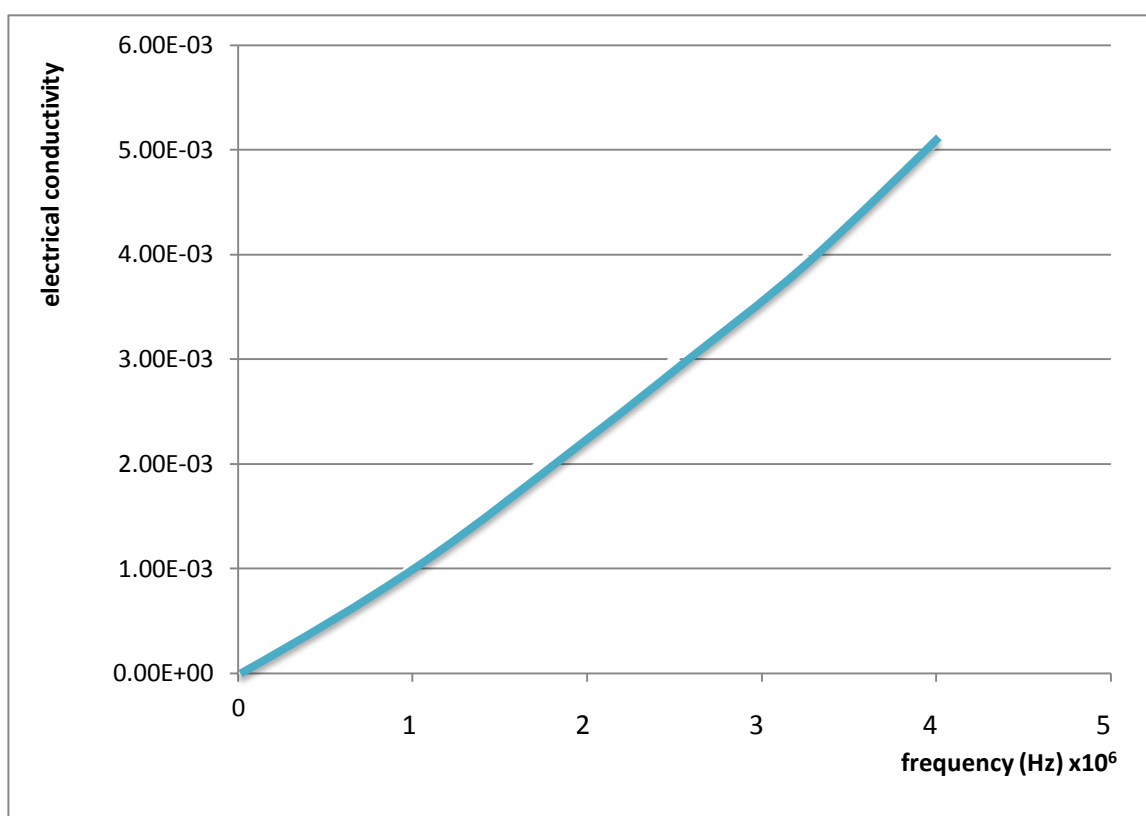


Figure (4-9): the variation of electrical conductivity with frequency for sample heated at (280 C°)

But when we heat the sample to (350°C) and the electrical conductivity is increased more than for sample prepared at (280°C) because the increase in temperature decrease the grain boundary and this get growth in the crystal and which lead to increase in electrical conductivity as in fig (4-10) [51] .

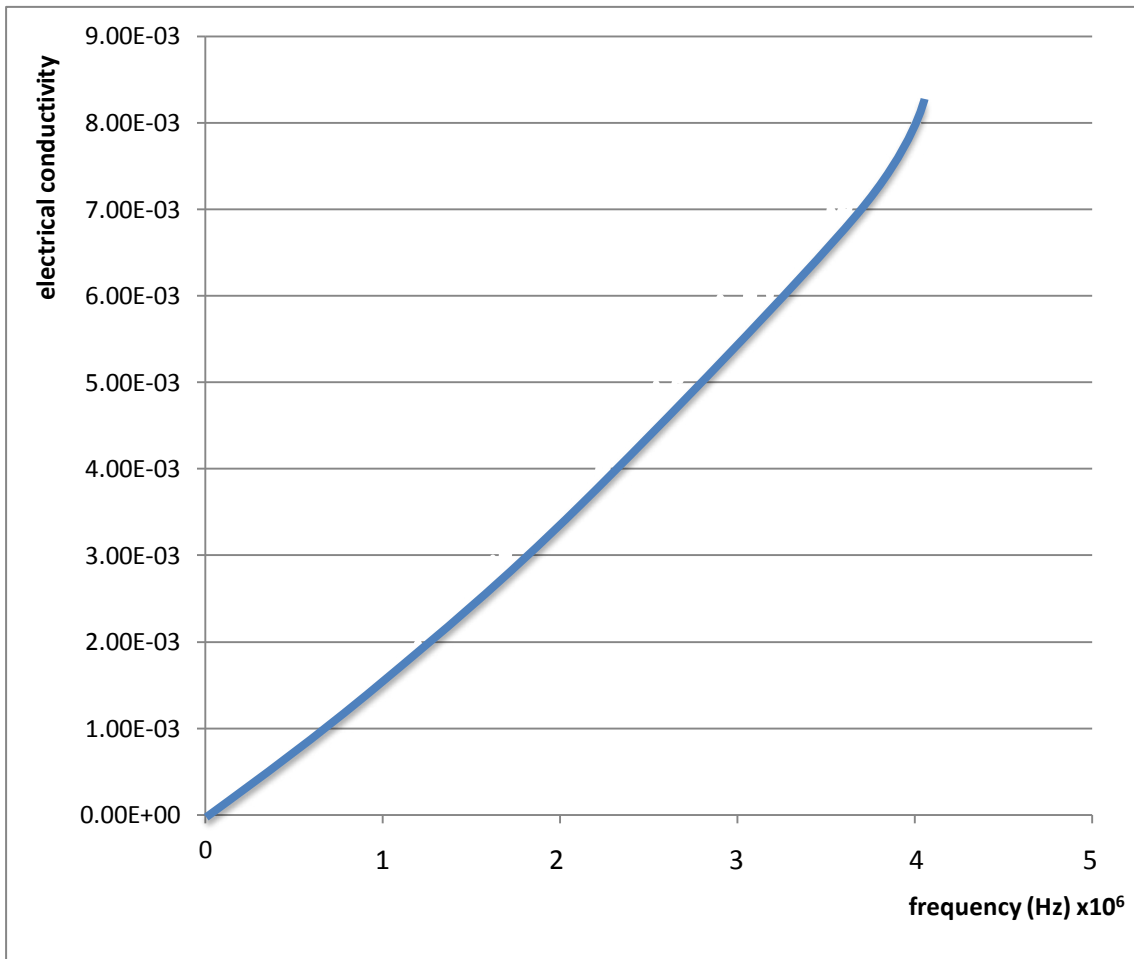


Figure (4-10): the variation of electrical conductivity with frequency for sample heated at (350 C°) and temperature

4.5.4. Electrical resistivity

The electrical resistivity of the sample have been computed for different frequencies in the range of (50 Hz to 5×10^6 Hz) and it is very high at low frequency and decrease gradually with increasing the frequency as shown in the figure (4-11) [52] for the sample at (280°C) .

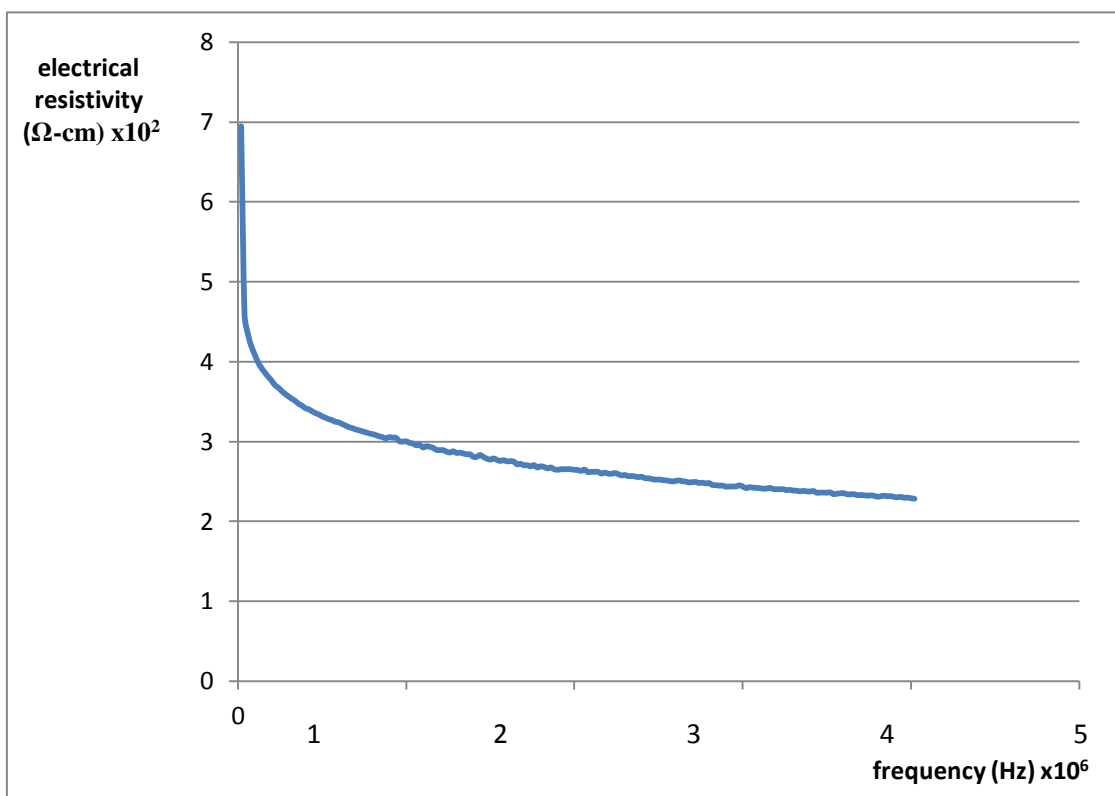


Figure (4-11): the variation of electrical resistivity with frequency for sample prepared at (280°C)

But when we burn the sample at (350°C) and the electrical resistivity is decreased more than for sample prepared at (280°C) this mean that the increase of temperature and frequency lead to increase in mobility which lead to decrease in the grain boundary and after that it get growth in crystal which lead to decrease in the resistivity and as in figure (4-12) [55] .

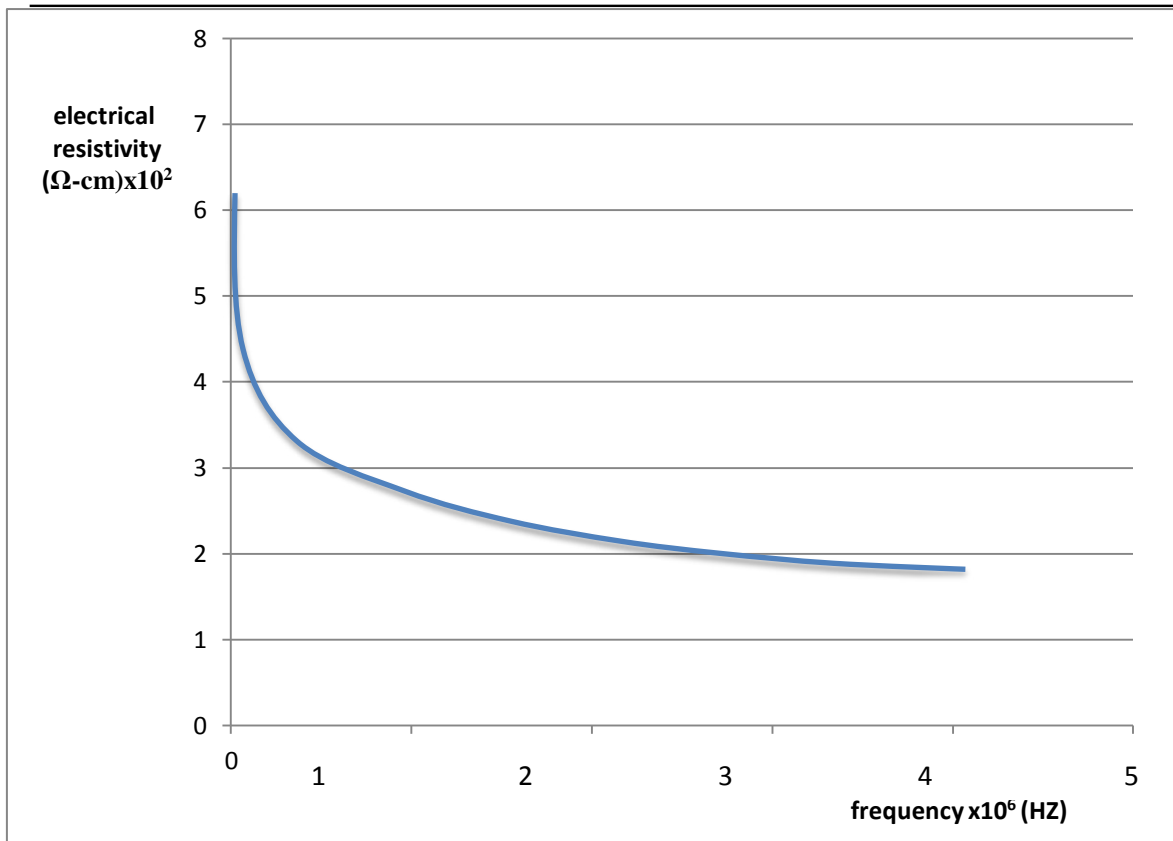


Figure (4-12): the variation of electrical resistivity with frequency for sample prepared at (350 C°)

4.5.5. Dielectric strength

The dielectric strength of the samples are measured at (5 kV/mm) it is observed a decrease in value of dielectric strength with increase in temperature as in table (4-5)

Table (4-5) Dielectric strength of alumina [62,93] .

Sample	Dielectric strength for sample calcined at 280°C	Dielectric strength for sample calcined at 350°C
Al ₂ O ₃	0.75 kV/mm	0.64 kV/mm

4.6. Conclusions

- 1- Sol – gel method is a very good method for synthesis (γ - alumina) with nano size particle .
- 2- The particle size of alumina increases with the increase in temperature in addition to the density whereas the porosity show the otherwise .
- 3- The hardness of alumina increases with the increase of temperature .
- 4- - The dielectric constant of alumina decreases with the increase of frequency, and decreases with the increase of temperature which makes it useful in insulator application for both lower and higher frequencies .
- 5- The tangent loss of alumina decreases with the increases of frequency, also decreases with the increase of temperature , so that it can be used in dielectrics.
- 6- The electrical resistivity of alumina decreases with the increases of frequency, and decreases with the increase of temperature , so that it can be used in electrical high frequency applications .
- 7- The electrical conductivity of alumina increases with the increases of frequency, also it increases with the increase of temperature .
- 8- The dielectric strength of alumina decrease with the increases of temperature .

4.7.Future work

- 1-The use of other techniques to prepare (γ - Alumina) with different nano-forms and studying its physical properties .
- 2- Sintering of alumina(γ , θ , β) after (1100) °C to convert to α -phase which is more stable phase for knowing its functional characteristic .
- 3- preparing of our prepared alumina composite for the use of high voltage electricity transformation .

References



References

- [1]. W. D. Kingery, H. K. Bowen and D. R. Uhlmann, John Wiley and Sons, Introduction to Ceramics, New York, (1975).
- [2]. T. A. Ring, Fundamentals of Ceramic Powder Processing and Synthesis, Academic Press, Inc. San Diego, 1st 96.
- [3]. Dream and Reality, G. Ondracek, 1. Hochschule, Composite Materials: 787-820, Advanced Structural Inorganic composites, edited by P. Vincenzini, Elsevier Science Publishers, Trieste, (1991) .
- [4]. C. K. Narula, Marcel Dekker, Ceramic Precursor Technology and its Application New York,(1995).
- [5]. C. Laurent, J. J. Demai, A. Rousset, K. R. Kannan and C. N. R. Rao, *J. Mater. Res* (1994), 9, 229.
- [6]. E. Breval, G. Dodds, C. G. Pantano, *Mater. Res. Bull.* 1985,20,1191.
- [7]. K. Niihara, T. Hirai, *Ceramics.* 26, 598, (1986).
- [8]. M. Sternitzke, *J. Eur. Ceram. Soc.* 17, 1061,(1997).
- [9]. A.N.Adamson, Alumina Production: Principles and Practice. Chemical Engineer, London, 239,156(1970), .
- [10]. K. Wefers, C. Misra, Alcoa, Oxides and Hydroxides of Aluminium, Laboratories, Pittsburgh (1987).
- [11]. R.H. Perry, Chemical Engineers Handbook, 6th ed ., McGraw-Hill, New , (1990)
- [12]. J. Tikkanen , K.A. Gross , C.C. Berndt, V. Pitkanen, J. Keskinen, S. Raghu, Rajala, J. Karthikeyan , Characteristics of the liquid flame sprayprocess ,*Surf . Coat . Technol.* 90 2010-2016(1997) .
- [13]. K.A. Evans, Manufacture of alumina and its use in ceramics and related applications, *Key Eng . Mater .* 122-124 489-526(1996) .

- [14]. M.N. Rittner , analysis of nanostructured materials , Am. Ceram. Soc. Bull . 81 (3) 33-36(2002) .
- [15]. L.C. Pathak, T.B. Singh, S. Das, A.K. Verma, P. Ramachandrarao, Effect of pH on the combustion synthesis of nano-crystalline alumina powder, Mater. Lett. 57 380–385(2002).
- [16] Y.Q. Wu, Y. Zhang, X. Huang, J. Guo, Preparation of plate like nano alpha alumina particles, Ceram. Int. 27 265–268(2001).
- [17]. J.M. Wu, Nano-sized amorphous alumina particles obtained by ball milling ZnO and Al powder mixture, Mater. Lett. 48 324–330(2001) .
- [18] T. Tani, L. M'adler, S.E. Pratsinis, Synthesis of zinc oxide/silica composite nanoparticles by flame spray pyrolysis, J. Mater. Sci. 37 4627–4632(2002).
- [19] J. Karthikeyan, C.C. Berndt, J. Tikkanen, J.Y. Wang, A.H. King, H. Herman, Nano material powders and deposits prepared by flame spray processing of liquid precursors, Nanostruct. Mater. 8 61–74(1997) .
- [20]. A.I.Y. Tok*, F.Y.C. Boey, X.L Zhao " Novel synthesis of Al₂O₃ nano-particles by flame spray pyrolysis " Journal of Materials Processing Technology 178 (2006) 270–273 .
- [21] Aluminum Oxide (Alumina) Ceramics & Properties-Marketech International Inc. School of Doctoral Studies (European Union) Journal – (2010)
- [22]. Janbey , Ranjank . Pati , Saad Tahir , Panchanan Pramanik " A new chemical route for the synthesis of nano –crystalline α -Al₂O₃ powder " Journal of the European Ceramic Society 21 2285-2289 (2001) .
- [23]. Cheng-Liang Huang a,* , Jun-Jie Wang a , Chi-Yuen Huang b "Sintering behavior and microwave dielectric properties of nano alpha-alumina " Materials Letters 59 ,3746 – 3749(2005).

[24]. Marie K. Tripp,* , Christoph Stampfer, David C. Miller, Thomas Helbling, Cari F. Herrmann, Christofer Hierold, Ken Gall, Steven M. George, Victor M. Bright " The mechanical properties of atomic layer deposited alumina for use in micro- and nano-electromechanical systems" Sensors and Actuators A 130–131, 419–429 (2006) .

[25]. Cheng-Liang Huangw and Jun-Jie Wang " Microwave Dielectric Properties of Sintered Alumina Using Nano-Scaled Powders of Alumina and TiO₂ " J. Am. Ceram. Soc., 90 [5] 1487–1493 (2007).

[26]. S. Cava a,* , S.M. Tebcherani a , I.A. Souza b , S.A. Pianaro a, C.A. Paskocimas c, E. Longob, J.A. Varela b " Structural characterization of phase transition of Al₂O₃ nano powders obtained by polymeric precursor method " Materials Chemistry and Physics 103 394–399(2007).

[27]. M. EDRISSI, R. NOROUZBEIGI* " Synthesis and characterization of alumina nano powders by combustion of nitrate-amino acid gels "Materials Science-Poland,. 25, No. 4, (2007).

[28]. R. Roman, T. Hernandez, and M. Gonzalez " Nano or micro grained alumina powder? A choose before sintering " Bol. Soc. Esp Ceram. V., 47,6,311-318 (2008) .

[29]. A.Boumaza, L.Favaro, J.Le´dion, G.Sattonnay, J.B.Brubach, P.Berthet, A.M.Huntz, P.Royc, R.Te´ tot Transition alumina phases induced by heat treatment of boehmite: An X-ray diffraction and infrared spectroscopy study, Journal of Solid State Chemistry 182 1171–1176 (2009) .

- [30]. Fatemeh Mirjalili, Hasmaliza Mo hamad* , Luqman Chuah , Preparation of nano-scale α -Al₂O₃ powder by the sol-gel Method Ceramics – Silikáty 55 (4) 378-383 (2011)
- [31]. M. R. Karim¹, M. A. Rahman, M. A. J. Miah, H. Ahmad*, M. Yanagisawa and M. Ito " Synthesis of γ -Alumina Particles and Surface Characterization " The Open Colloid Science Journal, (2011), 4, 32-36 .
- [32]. Rodica Rogojan, Ecaterina Andronescu, Cristina Ghitulica, Bogdan Ștefan Vasile ,Synthesis and Characterization of alumina nano-powder obtained by sol- gel method, U.P.B. Sci. Bull., Series B,73, Iss. 2,(2011).
- [33]. Omid Rahmanpour , Ahmad Shariati and Mohammad Reza Khosravi Nikou " new method for synthesis nano size γ -Al₂O₃ catalyst for Dehydration of Methanol to dimethyl Ether " International journal of chemical engineering and applications , 3, 2, April(2012).
- [34]. Sarojini Swain, Ram Avatar Sharma, Subhendu Bhattacharya, and Lokesh Chaudhary " Effects of Nano-silica/Nano-alumina on Mechanical and Physical Properties of Polyurethane Composites and Coatings " Transactions on electrical and electronic materials , No. 1, pp. 1-8, February 25,(2013) .
- [35]. Wenhui Yang, Ran Yi, Xu Yang, Man Xu, Sisi Hui, and Xiaolong Cao " Effect of Particle Size and Dispersion on Dielectric Properties in ZnO/Epoxy Resin Composites " Transactions on electrical and electronic materials, No. 3, pp. 116-120, June 25, (2012) .
- [36]. Akash Mohanty , V.K. Srivastava " Dielectric breakdown performance of alumina/epoxy resin nanocomposites under high voltage application " Materials and Design 47 , 711–716 (2013) .

[37]. K.G. Kalpana Sarojini , Siva V. Manoj, Pawan . Singh, T. Pradeep, Sarit K. Das, " Electrical conductivity of ceramic and metallic nanofluids" Colloids and Surfaces A: Physicochem. Eng. Aspects 417 , 39– 46 (2013).

[38] . Karen Davis " Material Review: Alumina (Al₂O₃)" Student of PhD in Chemical Engineering at the School of Doctoral Studies of the EU Square de Meeus 37-4th Floor 1000 Brussels, Belgium,(2010) .

39 . البصليي ، د.أحمد المصطفى، محمود، د.مظفر محمد، "المعادن والصخور"، جامعة بغداد،(1995).

40. يور يسوف.س، وآخرون، "هندسة المناجم"، دار مير للطباعة والنشر، موسكو، الاتحاد السوفيتي، (1978).

[41] R.Heslop and P.Robinson, "Inorganic Chemistry",3rd Edition, Elsevier publishing co., P.(774), (1967).

[42] E. Door, "Alumina", U.S.A, p.(10-218), (1984).

[43] . و.ريان ، "خواص المواد الخام السيراميكية"، ترجمة فاضل بندر عباس و آخرون، وزارة التعليم العالي والبحث العلمي، دار التقني للطباعة والنشر، (ص93-96)، (1986).

[44] F.H. Norton, "Fine ceramics Technology and applications". McGraw-Hill, Inc. (1970).

[45] S.Mrowec, "Defects and diffusion in solids", PWN-Polish, Scientific publishers, Warszawa, (1980).

[46] F.F. Lange, "J. Mater. Sci. "17, P.(247-254), (1982).

[47]. ISO 5017, ASTM C20, BS - 308, and SANS 5905 using mercury) (1902) .

[48]. M B Berger Cermalab : the importance and testing of density / porosity / permeability / pore size for refractories , The Southern African Institute of Mining and Metallurgy Refractories Conference (2010) .

[49]. Calce and the University of Maryland , 2001

- [50] U. Ghazanfar, "Preparation and characterization of ferrite materials for practical applications" university of the Punjab, Lahore, Pakistan (2005).
- [51] Smart, L. E.; Moore, E. A. Solid State Chemistry; CRC: New York, (2005).
- [52] E. Snelling, "Soft ferrites, properties and application" Butterworth and Co, (publishers) L.T.d, Londn, (1988).
- [53] K. Flaurance. " Complex oxides of the system Cu-Ni-Fe-O: synthesis parameters, phase formation and properties" The faculty of mathematics and natural sciences of the dresden university of technology, (2004).
- [54] Thomas Schroeder, "Physics of Dielectrics and DRAM", IHP Im Technologie park (25 15236) Frankfurt (Oder) Germany
- [55] د.النعيمي، علاء الدين، د.الجوادي، إبراهيم محمد علي الجوادي، د.قاسم محمود علي، "الفيزياء التطبيقية الحديثة"، الجامعة التكنولوجية، (ص179-181)، (1999).
- [56].Kwan Chi Kao, "Dielectric Phenomena In Solids With Emphasis on Physical Concepts of Electronic Processes", Elsevier, Inc, (2004).
- [57] Harinath Aireddy, " Investigation of Physico-Mechanical & Dielectrical Properties of Bio-Waste Reinforced Polymer Composites", National Institute of Technology, Rourkela, India, (2011).
- [58] W. Bolton, "Engineering Materials Technology", 3th edition, Prentice Hall Co., (1998).
- [59] S.A.S. Ali, Study " The Electromechanical Effects For Different Types of Glass " University of Baghdad, Master Thesis, (2010).
- [60] D. Halliday, R. Resnick , "Fundamentals of physics", John Wiley and sons, Inc, NEW YORK, P.(489-499), (1974).

- [61] J.C. Anderson, "Dielectrics", Chapman and Hall LTD, London, P.(39- 48,121-149),(1964).
- [62] B. Tareev, "Physics of dielectric materials", Mir publishers, Moscow, P.(101-145,174-202), (1979).
- [63] J.R.Reitz, "Foundation of electromagnetic theory", 3rd edition, Addison- Wesley, Inc, U.S.A, P.(75-113), (1979).
- [64] James D. Patterson, Bernard C. Bailey, " Solid State Physics Introduction to the Theory", Springer-Verlag Berlin Heidelberg ,(2007), p.(509), (2007).
- [65] Jalle, "An outline of polymer chemistry", Oliver and Boyed, Ltd, (1974).
- [66] M.C. Lovell, A.J. Aery, and M.W. Vernon, "Physical properties of materials", New York (1976).
- [67] R.A. Levy, "Principle of solid state physics", 4th edition, Academic press (1976).
- [68] H. Frohlich, "Theory of dielectrics", 1st edition, Oxford University Press. (1958).
- [69] S. Borowitz, and A. Beiser, "Essentials of Physics", 2nd edition, Addison-Wesley publishing Company, (1971).
- [70] William D. Callister, Jr., "Materials science and engineering introduction". John Wiley & Sons, p.(702-709), (2007).
- [71] Brian S. Mitchell, "An Introduction To Materials Engineering And Science", A John Wiley & Sons, Inc, P.(99-100), (2004).
- [72] Mailadil t.Sebastian, "dielectric materials for wireless communication", Elsevier, (2008).

73- الدكتور صبحي سعيد الراوي، الدكتور شاكر شاكر، الدكتور يوسف مولود حسن،
"فيزياء الحالة الصلبة"، وزارة التعليم العالي والبحث العلمي، جامعة الموصل، ص (299-
(1988)، (329)

[74] R.S. Khurmi, R.S. Sedha, "Material Science", 2nd edition, S. Chand and Company Ltd, (1989).

[75] Zuo-Guang Ye, "Handbook of dielectric, piezoelectric and ferroelectric materials Synthesis, properties and applications ", Wood head Publishing Limited, (2008).

[76] W.D. Gingery, H.K. Bowen, and D.R. Uhlmann, "Introduction to Ceramic", 2nd, Wiley New York, (1976).

[77] D. Halliday, R. Resnik, "Physics", Part (1,2), John Wily and Sons., Inc., (1962).

[78] Anthory, R. West, "Solid state chemistry and application", (1989).

[79] Abdullah A. H. Al-tamimi, "Preparation and Study of The Dielectric Properties of some Epoxy Composite ", Master Thesis, College of Education, University of Basrah, (2003).

[80] I.J. Mccolm, "Ceramic Science for materials Technologists", Leonard Hill, New York, (1983).

[81] Zinc–manganese ferrites, Ph.D. Thesis, Andhra University, Waltair, (1981).

[82] West, A. R. Solid State Chemistry and its Applications; John Wiley & Sons:Singapore, (1989).

- [83] Department of Defense Handbook, "Composite Materials Handbook", Vol.5, Ceramic Matrix Composites , U.S.A, Mil-Hdbk P.(27), (2002).
- [84] A. H.A. Al-Fouadi, "Dielectric Properties of Local Clay-Based Cordierite Ceramics", Al-Mustansiriyah University, Ph.D. Thesis, (2007).
- [85] K.J. Pascoe, "Properties of materials for electrical engineers", John wiley and sons, London, P.(173-194), (1974).
- [86] L. H. Van Vlack, "Elements of materials Science and engineering", 5th Edition, Addison-Wesley, (1987).
- [87] Peter Barber, Shiva Balasubramanian, Yogesh Anguchamy, Shushan Gong, Arief Wibowo, Hongsheng Gao, Harry J. Ploehn and Hans-Conrad zur Loye, "Polymer Composite and Nanocomposite Dielectric Materials for Pulse Power Energy Storage ", Materials, , p.(1697-1733), (2009).
- [88] L.A.Utracki, "Polymer Blends Handbook", Kluwer Academic Publishers Dordrecht, Boston,London, Vol. 1, P.(925), (2002).
- [89] Jean Sebastien Plante and Steven Dubowsky, "International Journal of Solids and Structures ".43, p.(7727-7751), (2006).
- [90] J. Stanek, "Electric melting of glass", Elsevier Scientific Comp, LTD, Amsterdam, P.(28-31) ,(1977),.
- [91] S. Felix, S.S. Sonja, "Industrial ceramics", John Wiley and sons, Inc, New York, U.S.A, P.(1050-1075), (1963).
- [92] I.bunget, P.Mihai, "Physics of solid dielectrics", Elsevier Oxford, P.(259-281), (1984).
- [93] E. Kuffel, W.S. Zaengl and J. Kuffel, "High Voltage Engineering Fundamentals", 2nd Edition., New Delhi, P. (369, 374, 382), (2000).

- [94] I. Kroschwitz, Jacqueline, "Electrical and Electronic Properties of Polymers: A State of Art Compendium", United State of America, P.(106- 107), (1988).
- [95] A.R. Blyth, "Electrical properties of polymers", Cambridge university press, London, P.(140-155), (1979).
- [96] العويسي، أحمد زيد عبيد، "دراسة التحمل لبعض المواد السيراميكية للجهد الكهربائي"، رسالة ماجستير، جامعة بغداد، (2004).
- [97] E. Kuffel, W. S. Zaengl, "High-Voltage Engineering" fundamentals, Toronto, P. (402-403), (1984).
- [98] E. kuffel, M. Abdullah, "High Voltage Engineering", Britain, P. (78-82), (1977).
- [99] أي كفل، ام - عبد الله، "هندسة الضغط العالي"، وزارة التعليم العالي والبحث العلمي، جامعة الموصل، ص (91-82)، (1982).
- [100] R.C. Buchanan, "perpratrneil of Engineering", New York, (1976).
- [101] D.V. Razevig, "High Voltage Engineering", Translated from Russian, M.P. Chourasia, Khanna publisher, New Delhi, India, P.(96-100), (1978).
- [102] Roland Coelho, "physics of Dielectrics" for engineering, New York, P. (143), (1979).
- [103] R. L. Timings, "Engineering Materials", , 2nd edition, Malaysia, P. (300). (2000).
- [104] T. Theivasanthi, M. Alagar " X-Ray Diffraction Studies of Copper Nano powder" Department of Physics, PACR Polytechnic College ,India (2010).
- [105] L.Jing, Z.Xu, J.Shang, X.Sun, W.Cai, H.Guo,"The preparation and characterization of ZnO ultrafine particles" Materials Science and Engineering A332 ,p.356–361,(2002).

[106]Y. Li "Synthesis of Copper(II) Oxide Particle and Detection of Photoelectrochemically Generated Hydrogen" Chemical Engineering, University of California, Davisin (2008).

الخلاصة

تم في هذا البحث تحضير مادة (الالومينا) طور كاما وبحجم 14.8 نانو بطريقة كيميائية هي (المحلول - جل) وقد تم فحص الخواص التركيبية بواسطة حيود الاشعة السينية حيث تم التوصل الى الحجم الحبيبي ومدى التبلور من خلال المطابقة مع البطاقة الدولية (JCPDS) No.(46. 1215) وايضا بواسطة المجهر الالكتروني الماسح الذي يبين ايضا الحجم الحبيبي واشكال الحبيبات وحجم المسامات وكذلك تمت دراسة الخواص الفيزيائية (الكثافة و المسامية والصلادة) بواسطة قاعدة ارخميدس وظهرت لنا القيمة التالية (1.692) (g/cm^3) ولوحظ بعد حرق المادة بدرجة (350°C) ان قيمة الكثافة تزداد لتصل الى (1.892) (g/cm^3) كذلك تم قياس المسامية بنفس الاسلوب (قاعدة ارخميدس) ولوحظ ان المسامية تقل من (6.8) الى (2.06) بعد الحرق اما بالنسبة للصلادة ازدادت قيمتها من (18 Gpa) الى (22Gpa) بعد عملية الحرق بدرجة حرارة (350). اما بالنسبة للخواص الكهربائية والعزلية استخدم جهاز (LCR METER) لقياس العينة ضمن مدى ترددي يتراوح بين (50 هرتز) الى 5ميكا هيرتز حيث لوحظ قيمة ثابت العزل تقل بازدياد التردد وكذلك المقاومة وظل الفقد . اما التوصيلية الكهربائية فانها تزداد بازدياد التردد اما زيادة درجة الحرارة تؤدي الى انخفاض في قيمة ثابت العزل الكهربائي وكذلك المقاومة الكهربائية وظل الفقد اما التوصيلية الكهربائية فانها تزداد بارتفاع درجة الحرارة ويتم قياس جهد الانهيار بواسطة جهاز قياس جهد الانهيار حيث لوحظ ان ارتفاع درجة الحرارة يؤدي الى نقصان في قيمة جهد الانهيار فانها تقل من (Kv/mm) 0.75 الى (Kv/mm) 0.64 بعد الحرق عند زيادة درجة الحرارة من (280 م) الى (350 م)



جمهورية العراق
وزارة التعليم العالي والبحث العلمي
جامعة ديالى
كلية العلوم / قسم الفيزياء

تحضير ودراسة الخصائص الفيزيائية للألومينا النانوية

رسالة مقدمة الى

مجلس كلية العلوم - جامعة ديالى وهي جزء من
متطلبات نيل درجة الماجستير علوم في الفيزياء

قديماً

نوار ثامر محمد الحمداني

بإشراف

أ.م.د. تحسين حسين مبارك أ.د. كريم هنيكش حسن

2014م

1435هـ